Available online at www.sciencedirect.com
SCIENCE DIRECT®
Spectrochimica Acta Part A 61 (2005) 2560–2575
SPECTROCHIMICA ACTA PART A
www.elsevier.com/locate/saa

# Theoretical prediction of gas-phase infrared spectra of imidazo[1,2-*a*]pyrazinediones and imidazo[1,2-*a*]imidazo[1,2-*d*]pyrazinediones derived from glycine

Flavio F. Contreras-Torres, Vladimir A. Basiuk*

*Instituto de Ciencias Nucleares, Universidad Nacional Autónoma de México, Circuito Exterior C.U., A. Postal 70-543, 04510 México D.F., Mexico*

Received 2 March 2004; accepted 29 September 2004

**Abstract**

Imidazo[1,2-*a*]pyrazine-3,6-diones and imidazo[1,2-*a*]imidazo[1,2-*d*]pyrazine-3,8-diones can be produced by pyrolysis of simple amino acids. While such bicyclic and tricyclic amidines were detected and characterized by IR spectroscopy for some α-substituted amino acids, the parent systems composed of glycine fragments are unknown up to now. IR spectra for five amidines derived from glycine were calculated by using different semi-empirical (PM3, AM1, MNDO and MINDO/3), HF, and hybrid DFT (B3LYP, B3P86 and B3PW91) methods in conjunction with 6-31G(*d*) basis set (for HF and DFT). Vibration frequencies in the experimental IR spectra were predicted based upon the B3LYP data, by correcting the calculated wavenumbers by a scaling factor of 0.959. The behavior of most characteristic bands ($\nu_{C=X}$, $\nu_{NH}$, etc.) and their shifts with respect to such bands in the spectra of alanine and α-aminoisobutyric acid derivatives studied before, are discussed. Performance of the semi-empirical methods was tested, bearing in mind possible future needs for IR spectra predictions for larger molecular systems of similar chemical nature; the use of MINDO/3 and MNDO is recommended. A basis set effect on the B3LYP fundamental vibration frequencies for hexahydroimidazo[1,2-*a*]pyrazine-3,6-dione was studied by varying Pople basis sets from minimal STO-3G to 6-311++G(*d*, *p*). No significant improvements were found beyond the 6-31G(*d*) basis set, which thus can be recommended to predict IR spectra for the amidines and similar molecules.


*Keywords:* Imidazo[1,2-*a*]pyrazinediones; Imidazo[1,2-*a*]imidazo[1,2-*d*]pyrazinediones; Glycine; HF; Hybrid DFT; Semi-empirical

## 1. Introduction

Despite amino acid and peptide chemistry is one of the best-explored areas of organic chemistry, there is an unusual class of amino acid/peptide derivatives, which remains very scarcely studied. Only a few examples are known of bicyclic amidine-type compounds composed of three α-amino acid residues (R = H, Alk), which belong to imidazo[1,2-*a*]pyrazines [1]:

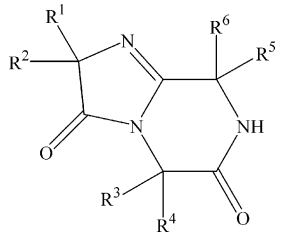


Although the formation of this bicyclic amidine system was first reported more than three decades ago [2,3], and afterwards several groups worked on different aspects of the bicyclic amidine chemistry [4–10], up to now less than 10 compounds of this class have been synthesized and characterized only. Synthetic approaches to them are based upon ei-

* Corresponding author. Tel.: +52 55 56 22 46 75; fax: +52 55 56 16 22 33.
*E-mail address:* basiuk@nuclecu.unam.mx (V.A. Basiuk).

1386-1425/$ – see front matter © 2004 Elsevier B.V. All rights reserved.
doi:10.1016/j.saa.2004.09.022

ther the use of tri- to pentapeptide precursors, in some cases along with rather drastic activating reagents such as phosphorus pentachloride or thionyl chloride [4,5,8], or inclusion into molecules of peptide starting material of sterically hindered α-amino acids, such as α-aminoisobutyric acid (Aib) [4,5,7,8] and α,α-diisopropylglycine [9,10].

By using the hyphenated technique of gas chromatography–Fourier transform infrared spectroscopy–mass spectrometry (GC–FTIR–MS), we further found that the bicyclic amidines can form as a result of amino acid pyrolysis. This can be observed when simple amino acids (e.g., α-aminoisobutyric acid, alanine, valine, norvaline and leucine) are pyrolyzed under temperature about 500 °C [11–13], or even under lower temperature of 200–300 °C in the presence of silica gel as a dehydration catalyst [12,14,15]. According to rough estimates, the yields of bicyclic amidines can reach 1–10% level in the latter case. The amidines form along with many other pyrolysis products and thus are extremely difficult to purify and study. Nevertheless, recently we were able to separate the α-aminoisobutyric acid derivative ($R^{1–6} = CH_3$) and to characterize its structure by X-ray diffraction [16]. Strasdeit et al. [17] reported on the bicyclic amidine detection in zinc and calcium complexes of valinate and isovalinate pyrolyzed at 320 °C.

Tricyclic imidazo[1,2-*a*]imidazo[1,2-*d*]pyrazine system is very close generically to the bicyclic imidazo[1,2-*a*]pyrazines. To the best of our knowledge, the only representative of such amino acid derivatives which was synthesized and characterized is the tricyclic amidine composed of four α-aminoisobutyric acid residues ($R^{1–8} = CH_3$) [4,5,7]:

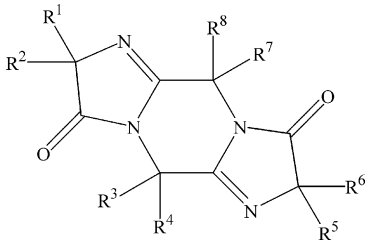


We also identified it in the α-aminoisobutyric acid pyrolyzates by means of GC–FTIR–MS [14,15]. Moreover, the corresponding tricyclic analog ($R^1$, $R^3$, $R^5$, $R^7 = CH_3$; $R^2$, $R^4$, $R^6$, $R^8 = H$) was found in alanine (Ala) pyrolyzates, by using the same technique [14,15].

The GC–FTIR–MS analysis has been the most abundant source of IR spectral information on the bicyclic and tricyclic amidines in the gas-phase. The value of this technique increases even further, taking into account that some of the amidines are present in complex pyrolytic mixtures as minor impurities, and cannot be separated and purified. Also, the amidines are not thermally stable compounds, and in situ decomposition in the GC column can be very notable for some of them (valine and leucine derivatives, for example). The above circumstances, along with the difficulties in the directed amidine synthesis, can explain why theoretical prediction of their IR spectra is of special interest.

A few years ago we have begun systematic studies in this area. As a first approach, we evaluated several semi-empirical methods (PM3, AM1, MNDO and MINDO/3) for calculating IR spectra of the alanine and α-aminoisobutyric acid amidine derivatives [18]. Then, geometric parameters and IR spectra of 2,2,5,5,8,8-hexamethylhexahydroimidazo[1,2-*a*]pyrazine-3,6-dione (i.e., α-aminoisobutyric acid bicyclic derivative) were computed by the HF, B3LYP, B3P86 and B3PW91 methods with the 6-31G(*d*) basis set [19]. We found a good correlation between the calculated and experimental vibration frequencies, with correlation coefficients higher than 0.9999 for the DFT methods, and 0.9995 for HF. Similarly, IR spectra of the bicyclic and tricyclic amidine derivatives of alanine were computed at the same theoretical levels [20], with the correlation coefficients of 0.9997 for all three DFT methods, and about 0.9992 for HF. In both works, the calculated absolute band intensities satisfactory matched the observed relative intensities. Thus, B3LYP, B3P86 and B3PW91 hybrid functionals, already used for IR spectra calculations of other classes of compounds (see for example [21–23]), worked well for the amidines of interest for us.

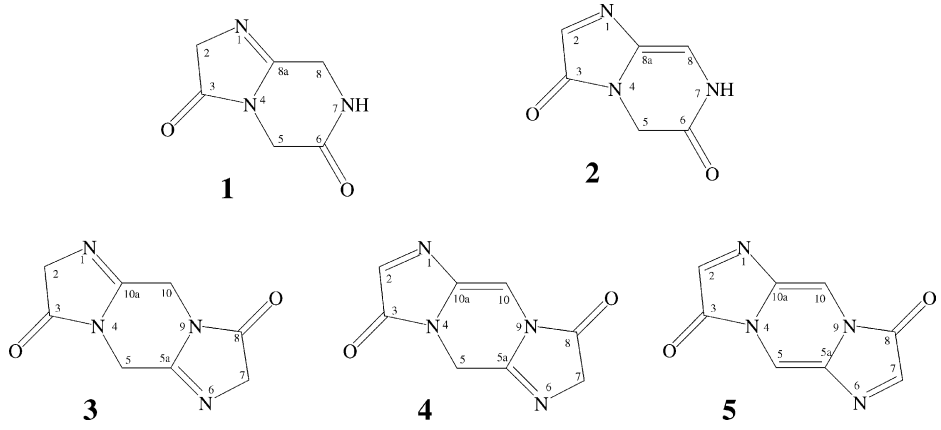


Fig. 1. Chemical structures and atomic numbering scheme for hexahydroimidazo[1,2-*a*]pyrazine-3,6-dione (**1**), tetrahydroimidazo[1,2-*a*]pyrazine-3,6-dione (**2**), hexahydroimidazo[1,2-*a*]imidazo[1,2-*d*]pyrazine-3,8-dione (**3**), tetrahydroimidazo[1,2-*a*]imidazo[1,2-*d*]pyrazine-3,8-dione (**4**), dihydroimidazo[1,2-*a*]imidazo[1,2-*d*]pyrazine-3,8-dione (**5**).

Table 1
Gas-phase vibration frequencies (in $cm^{-1}$) calculated directly by different methods and the corresponding scaled B3LYP values for hexahydroimidazo[1,2-*a*]pyrazine-3,6-dione (**1**)

| Mode | HF | B3LYP | B3P86 | B3PW91 | PM3 | AM1 | MNDO | MINDO/3 | Approximate description[a] | B3LYP scaled[b] |
|---|---|---|---|---|---|---|---|---|---|---|
| 1 | 68.0 | 61.3 | 61.2 | 61.1 | 47.5 | 36.8 | 31.9 | 42.7 | Rings deform | 58.8 |
| 2 | 117.3 | 110.1 | 111.0 | 110.6 | 100.2 | 94.7 | 86.0 | 90.6 | Rings deform | 105.6 |
| 3 | 163.5 | 155.6 | 157.3 | 156.8 | 134.0 | 106.3 | 102.7 | 149.9 | Rings deform; rock $C(8)H_2$ | 149.2 |
| 4 | 174.8 | 176.0 | 180.1 | 180.4 | 173.6 | 147.8 | 166.9 | 227.6 | Rings deform; rock $C(5)H_2$ | 168.8 |
| 5 | 266.9 | 243.6 | 243.7 | 243.6 | 242.4 | 262.5 | 251.3 | 241.6 | Rings deform; rock $C(2)H_2$ | 233.6 |
| 6 | 286.1 | 266.0 | 266.2 | 265.6 | 249.7 | 265.4 | 278.2 | 243.0 | Rings deform; rock $C(2)H_2$, $C(8)H_2$ | 255.1 |
| 7 | 449.4 | 414.1 | 414.4 | 414.1 | 401.2 | 438.1 | 419.8 | 383.8 | Pyrazine ring deform; rock $C(2)H_2$ | 397.1 |
| 8 | 462.9 | 429.5 | 431.3 | 430.5 | 415.6 | 442.7 | 447.4 | 397.5 | Rings deform | 411.9 |
| 9 | 545.4 | 500.9 | 501.4 | 501.3 | 485.0 | 467.7 | 499.2 | 475.4 | Rock $C(5)H_2$; NH deform out-of-plane | 480.3 |
| 10 | 582.0 | 525.9 | 525.6 | 525.5 | 520.3 | 522.4 | 543.3 | 492.5 | All $CH_2$ rock; NH deform out-of-plane | 504.3 |
| 11 | 589.9 | 536.3 | 539.7 | 539.4 | 542.9 | 542.3 | 562.9 | 501.0 | All $CH_2$ rock; NH deform out-of-plane | 514.4 |
| 12 | 637.5 | 592.1 | 596.3 | 595.4 | 553.3 | 573.7 | 576.1 | 520.0 | All $CH_2$ rock; NH deform out-of-plane | 567.9 |
| 13 | 667.5 | 614.2 | 617.7 | 616.8 | 578.0 | 605.4 | 603.0 | 547.0 | All $CH_2$ rock; NH deform out-of-plane | 589.0 |
| 14 | 713.1 | 650.0 | 654.5 | 653.4 | 632.6 | 620.1 | 606.9 | 585.1 | All $CH_2$ rock; NH deform out-of-plane | 623.3 |
| 15 | 761.0 | 701.3 | 706.8 | 705.3 | 674.9 | 733.4 | 688.2 | 609.7 | Rings deform | 672.5 |
| 16 | 796.9 | 739.5 | 747.1 | 745.1 | 738.2 | 814.7 | 778.6 | 671.9 | Rings deform | 709.2 |
| 17 | 878.1 | 808.1 | 817.9 | 815.9 | 810.1 | 903.0 | 893.0 | 828.5 | Rings deform | 774.9 |
| 18 | 921.6 | 849.7 | 857.9 | 855.6 | 887.5 | 981.5 | 1002.6 | 859.6 | Rings deform | 814.9 |
| 19 | 1077.2 | 977.0 | 975.3 | 974.8 | 900.2 | 990.7 | 1021.7 | 864.9 | All $CH_2$ rock; NH deform out-of-plane | 937.0 |
| 20 | 1098.1 | 988.0 | 991.5 | 990.4 | 909.6 | 994.0 | 1031.7 | 878.5 | All $CH_2$ rock; NH deform out-of-plane | 947.5 |
| 21 | 1106.3 | 1007.4 | 1007.2 | 1006.4 | 917.2 | 1008.2 | 1035.5 | 954.0 | Stretch C(2)N; rock $C(5)H_2$, $C(8)H_2$ | 966.0 |
| 22 | 1149.2 | 1043.2 | 1051.9 | 1050.3 | 992.5 | 1072.4 | 1131.0 | 999.1 | Rings deform; rock $C(5)H_2$, $C(8)H_2$ | 1000.5 |
| 23 | 1151.2 | 1057.3 | 1073.2 | 1070.7 | 998.9 | 1092.3 | 1154.3 | 1014.1 | Rings deform | 1014.0 |
| 24 | 1178.8 | 1084.7 | 1098.7 | 1097.3 | 1042.5 | 1148.9 | 1225.8 | 1094.8 | Stretch C(8)N | 1040.2 |
| 25 | 1252.8 | 1138.7 | 1155.9 | 1152.0 | 1048.1 | 1179.9 | 1239.4 | 1096.3 | Rings deform | 1092.0 |
| 26 | 1304.6 | 1190.8 | 1191.3 | 1191.6 | 1068.9 | 1195.3 | 1254.0 | 1121.5 | Twist $C(2)H_2$ | 1142.0 |
| 27 | 1347.4 | 1231.9 | 1234.8 | 1234.9 | 1084.7 | 1243.3 | 1271.2 | 1136.0 | Wagging $C(2)H_2$; twist $C(5)H_2$ | 1181.4 |
| 28 | 1366.6 | 1254.2 | 1256.3 | 1256.3 | 1115.9 | 1279.9 | 1305.9 | 1155.8 | Twist $C(8)H_2$ | 1202.8 |
| 29 | 1396.7 | 1274.3 | 1276.7 | 1276.3 | 1207.2 | 1323.5 | 1378.1 | 1206.1 | Wagging $C(2)H_2$; twist $C(5)H_2$, $C(8)H_2$ | 1222.1 |
| 30 | 1436.1 | 1310.5 | 1313.7 | 1313.0 | 1274.5 | 1332.5 | 1411.3 | 1264.8 | All $CH_2$ wagging | 1256.7 |
| 31 | 1492.4 | 1350.7 | 1361.3 | 1359.6 | 1298.5 | 1360.3 | 1428.9 | 1297.4 | All $CH_2$ wagging | 1295.4 |
| 32 | 1506.6 | 1358.5 | 1373.4 | 1370.2 | 1313.6 | 1366.2 | 1434.6 | 1308.5 | All $CH_2$ wagging | 1302.8 |
| 33 | 1549.3 | 1404.5 | 1412.9 | 1411.2 | 1332.5 | 1374.2 | 1440.1 | 1310.9 | NH deform in-plane | 1347.0 |
| 34 | 1574.9 | 1445.7 | 1457.1 | 1456.3 | 1343.2 | 1453.8 | 1488.8 | 1334.8 | All $CH_2$ wagging; stretch C(8a)N(4) | 1386.4 |
| 35 | 1602.3 | 1468.5 | 1465.5 | 1463.3 | 1354.9 | 1492.2 | 1507.6 | 1350.9 | Scissors $C(2)H_2$ | 1408.3 |
| 36 | 1636.0 | 1494.4 | 1496.2 | 1495.6 | 1386.7 | 1508.0 | 1534.1 | 1391.1 | Scissors $C(5)H_2$, $C(8)H_2$ | 1433.1 |
| 37 | 1647.3 | 1518.5 | 1514.2 | 1513.8 | 1405.6 | 1630.2 | 1638.7 | 1437.9 | Scissors $C(5)H_2$, $C(8)H_2$ | 1456.2 |
| 38 | 1659.0 | 1535.6 | 1535.5 | 1534.4 | 1461.2 | 1647.4 | 1649.6 | 1497.1 | Scissors $C(5)H_2$, $C(8)H_2$ | 1472.6 |
| 39 | 1930.0 | 1722.4 | 1741.7 | 1737.4 | 1814.5 | 1837.4 | 1880.9 | 1735.8 | Stretch C=N | 1651.8 |
| 40 | 1989.1 | 1813.8 | 1835.5 | 1831.4 | 1927.4 | 2005.5 | 2090.7 | 1880.8 | Stretch C(6)=O | 1739.4 |
| 41 | 2026.1 | 1844.2 | 1866.0 | 1862.0 | 1989.5 | 2086.0 | 2166.8 | 1946.0 | Stretch C(3)=O | 1768.6 |
| 42 | 3201.4 | 3006.2 | 3022.5 | 3017.8 | 2903.6 | 2945.4 | 3182.5 | 3280.5 | Stretch asymmetric $C(8)H_2$ | 2883.0 |
| 43 | 3236.1 | 3050.0 | 3066.0 | 3061.4 | 2916.2 | 2954.8 | 3195.5 | 3309.6 | Stretch asymmetric $C(5)H_2$ | 2924.9 |
| 44 | 3247.1 | 3071.4 | 3084.6 | 3080.2 | 2967.7 | 3016.7 | 3237.2 | 3309.9 | Stretch symmetric $C(2)H_2$ | 2945.5 |
| 45 | 3287.8 | 3107.4 | 3125.1 | 3120.9 | 2978.0 | 3020.5 | 3253.3 | 3325.8 | Stretch asymmetric $C(2)H_2$ | 2980.0 |
| 46 | 3319.6 | 3130.1 | 3146.0 | 3141.8 | 2988.4 | 3028.2 | 3253.6 | 3369.1 | Stretch asymmetric $C(8)H_2$ | 3001.7 |
| 47 | 3326.3 | 3134.0 | 3148.6 | 3145.7 | 3026.6 | 3081.0 | 3295.6 | 3379.6 | Stretch asymmetric $C(5)H_2$ | 3005.5 |
| 48 | 3852.0 | 3597.9 | 3625.7 | 3623.4 | 3369.8 | 3470.6 | 3570.8 | 3574.2 | Stretch NH | 3450.4 |

[a] Based on B3LYP.
[b] B3LYP scaled by sf = 0.959 [20].

Based on the comparison of theoretical and experimental data, for future IR spectral predictions for unknown compounds of this class, we recommended uniform scaling factors of 0.897, 0.959, 0.954 and 0.955 for HF, B3LYP, B3P86 and B3PW91, respectively [20].

Such unknown compounds can be best exemplified by the bi- and tricyclic amidines derived from glycine (Gly). Neither other research groups nor we ourselves ever synthesized or detected them by any method. This fact is striking, since glycine molecule as the simplest α-amino acid representative does not have any α-substituent, and logically should exhibit the highest reactivity in the condensation reactions producing amidine systems. On the contrary, even the yields of piperazine-2,5-dione

Table 2
Gas-phase vibration frequencies (in $cm^{-1}$) calculated directly by different methods and the corresponding scaled B3LYP values for tetrahydroimidazo[1,2-*a*]pyrazine-3,6-dione (**2**)

| Mode | HF | B3LYP | B3P86 | B3PW91 | PM3 | AM1 | MNDO | MINDO/3 | Approximate description[a] | B3LYP scaled[b] |
|---|---|---|---|---|---|---|---|---|---|---|
| 1 | 69.3 | 65.4 | 65.1 | 65.5 | 80.0 | 19.5 | 32.5 | 71.1 | Rock C(5)$H_2$ | 62.7 |
| 2 | 121.9 | 123.0 | 123.9 | 123.6 | 94.0 | 67.0 | 81.9 | 92.4 | Rings deform | 118.0 |
| 3 | 137.8 | 146.4 | 150.2 | 151.8 | 191.9 | 106.7 | 121.6 | 210.1 | Rings deform | 140.4 |
| 4 | 258.3 | 231.3 | 230.9 | 231.2 | 221.3 | 248.2 | 213.6 | 239.4 | Rings deform | 221.8 |
| 5 | 283.8 | 269.4 | 271.0 | 270.3 | 259.2 | 261.9 | 275.8 | 241.5 | Rings deform | 258.3 |
| 6 | 465.1 | 427.6 | 427.4 | 427.4 | 362.8 | 385.6 | 353.9 | 352.8 | Pyrazine ring deform; C(6)=O deform in-plane | 410.0 |
| 7 | 483.1 | 450.7 | 454.4 | 453.5 | 404.0 | 442.8 | 439.4 | 387.5 | Rings deform | 432.2 |
| 8 | 495.4 | 459.8 | 462.3 | 461.6 | 424.5 | 487.5 | 451.1 | 416.7 | Pyrazine ring deform | 441.0 |
| 9 | 546.2 | 531.2 | 532.7 | 533.0 | 472.2 | 494.4 | 475.7 | 486.8 | Rock C(5)$H_2$; NH deform in-plane | 509.5 |
| 10 | 575.5 | 532.7 | 536.0 | 535.6 | 517.4 | 563.3 | 564.7 | 491.6 | Pyrazine ring deform; C(3)=O deform in-plane | 510.9 |
| 11 | 672.5 | 626.6 | 629.3 | 628.3 | 551.9 | 572.5 | 565.5 | 526.7 | Imidazole ring deform; C(6)=O deform in-plane | 600.9 |
| 12 | 679.0 | 632.7 | 637.0 | 636.1 | 570.5 | 581.4 | 585.6 | 529.6 | Rings deform | 606.7 |
| 13 | 691.4 | 655.8 | 661.8 | 660.9 | 594.1 | 635.8 | 617.7 | 593.1 | Rock C(5)$H_2$; NH deform out-of-plane | 628.9 |
| 14 | 782.5 | 728.7 | 734.1 | 732.6 | 663.7 | 698.2 | 694.8 | 601.7 | Rings deform | 698.9 |
| 15 | 812.4 | 734.1 | 736.8 | 736.1 | 691.1 | 764.4 | 723.2 | 627.9 | Imidazole ring deform; C(8)H deform out-of-plane | 704.0 |
| 16 | 820.1 | 763.2 | 771.0 | 768.9 | 753.7 | 848.9 | 810.2 | 683.9 | Rings deform | 731.9 |
| 17 | 869.9 | 810.0 | 819.8 | 817.8 | 830.4 | 876.5 | 909.7 | 755.3 | Rings deform | 776.8 |
| 18 | 929.3 | 818.3 | 820.4 | 819.8 | 884.2 | 922.1 | 939.0 | 782.6 | C(8)H deform out-of-plane | 784.7 |
| 19 | 956.6 | 857.7 | 865.5 | 863.2 | 894.8 | 929.6 | 983.7 | 846.0 | Rings deform | 822.5 |
| 20 | 1028.8 | 893.6 | 894.4 | 894.0 | 898.2 | 984.5 | 1008.3 | 863.5 | C(2)H deform out-of-plane | 857.0 |
| 21 | 1119.4 | 1015.1 | 1011.4 | 1010.9 | 914.6 | 998.8 | 1022.8 | 960.9 | Rock C(5)$H_2$ | 973.5 |
| 22 | 1179.0 | 1086.6 | 1095.5 | 1093.6 | 1144.4 | 1098.5 | 1158.5 | 1005.0 | Wagging C(5)$H_2$; C(2)H, C(8)H deform in-plane | 1042.0 |
| 23 | 1193.3 | 1118.7 | 1128.8 | 1127.7 | 1020.9 | 1145.7 | 1242.9 | 1116.3 | NH, C(8)H deform in-plane | 1072.9 |
| 24 | 1286.9 | 1179.4 | 1195.3 | 1192.0 | 1046.3 | 1168.9 | 1245.8 | 1120.6 | Rings deform; C(8)H deform in-plane | 1131.1 |
| 25 | 1341.3 | 1220.4 | 1233.2 | 1231.3 | 1091.5 | 1237.0 | 1303.6 | 1150.4 | All C-N stretch; wagging C(5)$H_2$; C(2)H deform in-plane | 1170.3 |
| 26 | 1363.8 | 1249.5 | 1249.3 | 1250.5 | 1128.2 | 1300.0 | 1323.1 | 1164.3 | Twist C(5)$H_2$ | 1198.3 |
| 27 | 1409.7 | 1292.5 | 1305.1 | 1303.1 | 1229.0 | 1327.5 | 1404.9 | 1251.0 | Wagging C(5)$H_2$; NH deform in-plane | 1239.5 |
| 28 | 1452.6 | 1334.7 | 1347.2 | 1344.7 | 1277.3 | 1368.3 | 1435.7 | 1299.8 | C(2)H deform in-plane | 1279.9 |
| 29 | 1486.6 | 1343.9 | 1352.7 | 1350.4 | 1307.6 | 1440.9 | 1460.9 | 1306.1 | Wagging C(5)$H_2$; C(8)H deform in-plane | 1288.8 |
| 30 | 1536.3 | 1385.2 | 1395.6 | 1393.4 | 1342.1 | 1448.1 | 1493.5 | 1335.1 | Wagging C(5)$H_2$ | 1328.4 |
| 31 | 1595.6 | 1462.7 | 1479.5 | 1476.6 | 1350.7 | 1484.4 | 1525.0 | 1342.5 | Wagging C(5)$H_2$; C(8)H deform in-plane | 1402.7 |
| 32 | 1619.4 | 1479.5 | 1487.7 | 1487.0 | 1401.3 | 1607.9 | 1614.0 | 1409.8 | NH deform in-plane | 1418.8 |
| 33 | 1644.8 | 1523.1 | 1519.6 | 1519.0 | 1424.8 | 1640.0 | 1651.4 | 1449.7 | Scissors C(5)$H_2$ | 1460.7 |
| 34 | 1806.2 | 1562.6 | 1578.3 | 1576.2 | 1756.4 | 1785.3 | 1800.3 | 1676.7 | Stretch C=N | 1498.6 |
| 35 | 1951.9 | 1751.1 | 1767.6 | 1763.4 | 1869.2 | 1875.9 | 1874.4 | 1798.6 | Stretch C=C | 1679.3 |
| 36 | 1994.8 | 1805.9 | 1828.3 | 1824.1 | 1939.0 | 2016.2 | 2095.4 | 1883.6 | Stretch C(3)=O | 1731.8 |
| 37 | 2008.6 | 1817.7 | 1839.0 | 1834.9 | 1987.9 | 2081.6 | 2158.8 | 1929.7 | Stretch C(6)=O | 1743.2 |
| 38 | 3252.8 | 3060.5 | 3073.9 | 3070.3 | 2917.1 | 2948.8 | 3190.9 | 3298.0 | Stretch symmetric C(5)$H_2$ | 2935.0 |
| 39 | 3295.8 | 3091.5 | 3109.8 | 3106.5 | 2990.8 | 3022.1 | 3249.8 | 3317.2 | Stretch asymmetric C(5)$H_2$ | 2964.7 |
| 40 | 3427.7 | 3244.9 | 3259.6 | 3254.9 | 3028.5 | 3151.7 | 3409.4 | 3455.3 | Stretch C(2)H | 3111.9 |
| 41 | 3457.2 | 3276.5 | 3289.6 | 3285.4 | 3081.6 | 3205.2 | 3439.7 | 3461.0 | Stretch C(8)H | 3142.1 |
| 42 | 3872.3 | 3610.1 | 3634.2 | 3632.5 | 3381.3 | 3460.4 | 3579.7 | 3591.0 | Stretch NH | 3462.1 |

[a] Based on B3LYP.
[b] B3LYP scaled by sf = 0.959 [20].

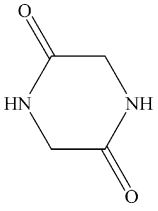


which is primary condensation product and direct amidine precursor, are unexpectedly low as compared to the piperazine-2,5-dione yields for other simple amino acids [24–26].

The amidine derivatives of glycine are of great interest from the point of view of future experimental studies of amino acid pyrolysis, where they might manifest themselves, and as central compounds for the whole amidine chemistry. Any relevant IR spectral information would be useful in their detection and characterization. The above considerations motivated our present work, in which we calculated IR spectra of the amidines by different semi-empirical (PM3, AM1, MNDO and MINDO/3), HF, and hybrid DFT (B3LYP, B3P86 and B3PW91) methods. The compounds studied were not only bicyclic amidine **1** and tricyclic amidine **3** (Fig. 1) expected to be direct condensation products of glycine, but also possible products of further dehydrogenation, **2**, **4** and **5** (the latter process was observed in the case of alanine, valine and leucine pyrolysis [11–14]).

## 2. Calculation details

All ab initio and DFT calculations were performed with the Gaussian 98W program package [27]. The structures were fully optimized (default convergence criteria) and normal modes were calculated with the HF, B3LYP, B3P86 and

Table 3
Gas-phase vibration frequencies (in $cm^{-1}$) calculated directly by different methods and the corresponding scaled B3LYP values for hexahydroimidazo[1,2-*a*]imidazo[1,2-*d*]pyrazine-3,8-dione (**3**)

| Mode | HF | B3LYP | B3P86 | B3PW91 | PM3 | AM1 | MNDO | MINDO/3 | Approximate description[a] | B3LYP scaled[b] |
|---|---|---|---|---|---|---|---|---|---|---|
| 1 | 51.7 | 48.3 | 46.4 | 46.6 | 19.5 | 33.0 | 20.2 | 19.0 | Pyrazine ring deform | 46.3 |
| 2 | 93.8 | 89.7 | 90.3 | 89.8 | 67.9 | 73.0 | 63.7 | 65.2 | Rings deform | 86.0 |
| 3 | 145.4 | 135.6 | 136.3 | 136.2 | 108.0 | 111.6 | 100.3 | 113.0 | Rings deform | 130.0 |
| 4 | 176.0 | 177.0 | 180.4 | 180.9 | 159.0 | 139.0 | 166.2 | 208.9 | Rings deform | 169.8 |
| 5 | 187.8 | 188.0 | 188.4 | 189.1 | 170.9 | 166.6 | 169.2 | 224.8 | Rings deform | 180.3 |
| 6 | 249.0 | 229.8 | 230.3 | 229.8 | 216.8 | 240.8 | 235.5 | 224.8 | Rock $C(2)H_2$, $C(7)H_2$ | 220.3 |
| 7 | 271.0 | 249.2 | 247.9 | 248.0 | 242.9 | 264.5 | 247.3 | 242.3 | Rings deform | 238.9 |
| 8 | 283.5 | 264.8 | 265.4 | 265.1 | 243.1 | 269.0 | 249.2 | 243.0 | Rings deform | 254.0 |
| 9 | 286.7 | 268.5 | 268.2 | 267.9 | 253.9 | 276.7 | 288.8 | 252.2 | All $CH_2$ rock | 257.5 |
| 10 | 444.0 | 414.0 | 415.6 | 414.9 | 403.5 | 450.3 | 424.0 | 376.8 | Pyrazine ring deform | 397.0 |
| 11 | 554.6 | 509.0 | 511.0 | 510.6 | 479.0 | 519.5 | 537.4 | 473.1 | Rings deform | 488.2 |
| 12 | 566.9 | 518.3 | 517.7 | 517.9 | 499.5 | 523.2 | 538.5 | 474.5 | Rings deform | 497.0 |
| 13 | 579.4 | 524.3 | 527.6 | 527.2 | 516.0 | 525.2 | 542.9 | 475.0 | Rings deform | 502.8 |
| 14 | 587.7 | 530.7 | 531.8 | 531.7 | 529.2 | 546.0 | 547.0 | 477.7 | Rings deform | 508.9 |
| 15 | 659.3 | 603.1 | 606.2 | 605.4 | 565.1 | 594.3 | 584.8 | 529.7 | Rings deform | 578.4 |
| 16 | 675.6 | 626.5 | 631.3 | 630.2 | 578.6 | 617.6 | 611.6 | 546.2 | Rings deform | 600.8 |
| 17 | 703.0 | 640.2 | 644.8 | 644.0 | 587.3 | 665.6 | 629.9 | 562.1 | Rings deform | 614.0 |
| 18 | 719.5 | 660.4 | 666.3 | 664.9 | 631.9 | 701.3 | 651.6 | 563.5 | Rings deform | 633.4 |
| 19 | 782.7 | 725.9 | 729.6 | 728.0 | 687.0 | 759.0 | 719.7 | 599.9 | Rings deform | 696.1 |
| 20 | 791.1 | 728.6 | 739.4 | 737.6 | 719.8 | 810.2 | 767.9 | 646.2 | Rings deform | 698.7 |
| 21 | 833.3 | 775.6 | 781.7 | 779.9 | 777.6 | 869.9 | 863.5 | 799.1 | Rings deform | 743.8 |
| 22 | 881.9 | 807.8 | 816.0 | 814.2 | 848.1 | 948.5 | 954.8 | 862.4 | Rings deform | 774.7 |
| 23 | 1071.3 | 972.5 | 970.6 | 970.0 | 894.1 | 986.9 | 1025.1 | 862.6 | All $CH_2$ rock | 932.6 |
| 24 | 1074.6 | 982.5 | 978.7 | 978.2 | 895.5 | 988.5 | 1029.7 | 872.4 | All $CH_2$ rock | 942.2 |
| 25 | 1094.9 | 983.1 | 990.6 | 989.6 | 909.9 | 992.3 | 1032.0 | 878.3 | All $CH_2$ rock | 942.8 |
| 26 | 1099.1 | 989.0 | 994.5 | 992.5 | 910.2 | 996.7 | 1032.6 | 898.8 | All $CH_2$ rock | 948.4 |
| 27 | 1099.2 | 999.2 | 1000.3 | 999.3 | 971.4 | 1071.8 | 1108.6 | 994.5 | Rock $C(5)H_2$, $C(10)H_2$ | 958.3 |
| 28 | 1137.1 | 1033.3 | 1053.1 | 1050.7 | 998.0 | 1072.4 | 1144.9 | 1008.6 | Rock $C(5)H_2$, $C(10)H_2$; wagging $C(2)H_2$, $C(7)H_2$ | 991.0 |
| 29 | 1156.5 | 1056.6 | 1066.2 | 1064.6 | 998.8 | 1080.6 | 1153.7 | 1013.5 | Rock $C(5)H_2$, $C(10)H_2$; wagging $C(2)H_2$, $C(7)H_2$ | 1013.2 |
| 30 | 1157.6 | 1061.2 | 1079.2 | 1076.4 | 1001.5 | 1100.1 | 1153.9 | 1014.0 | Rock $C(5)H_2$, $C(10)H_2$; wagging $C(2)H_2$, $C(7)H_2$ | 1017.7 |
| 31 | 1232.0 | 1118.5 | 1138.9 | 1134.3 | 1035.3 | 1154.7 | 1237.6 | 1080.5 | Wagging $C(5)H_2$, $C(10)H_2$; C=O deform in-plane | 1072.7 |
| 32 | 1253.7 | 1141.6 | 1155.3 | 1151.9 | 1036.2 | 1159.9 | 1238.7 | 1109.4 | Rock $C(5)H_2$, $C(10)H_2$; C=O deform in-plane | 1094.8 |
| 33 | 1305.0 | 1191.5 | 1191.7 | 1192.1 | 1055.7 | 1194.3 | 1247.2 | 1115.0 | Twist $C(2)H_2$, $C(7)H_2$ | 1142.6 |
| 34 | 1305.3 | 1191.5 | 1191.7 | 1192.2 | 1074.0 | 1196.4 | 1249.5 | 1120.1 | Twist $C(2)H_2$, $C(7)H_2$ | 1142.7 |
| 35 | 1328.6 | 1216.0 | 1223.4 | 1222.4 | 1116.0 | 1243.0 | 1269.7 | 1143.4 | Wagging $C(2)H_2$, $C(7)H_2$ | 1166.2 |
| 36 | 1340.6 | 1223.6 | 1223.9 | 1224.0 | 1116.2 | 1284.3 | 1302.3 | 1158.4 | Wagging $C(2)H_2$, $C(7)H_2$ | 1173.4 |
| 37 | 1400.1 | 1278.4 | 1280.4 | 1280.1 | 1194.9 | 1322.3 | 1376.9 | 1205.4 | Wagging $C(2)H_2$, $C(7)H_2$; twist $C(5)H_2$, $C(10)H_2$ | 1226.0 |
| 38 | 1405.4 | 1279.1 | 1282.3 | 1281.7 | 1238.0 | 1327.7 | 1381.9 | 1225.3 | Wagging $C(2)H_2$, $C(7)H_2$; twist $C(5)H_2$, $C(10)H_2$ | 1226.7 |
| 39 | 1449.0 | 1313.6 | 1313.9 | 1313.6 | 1275.2 | 1337.8 | 1412.4 | 1281.9 | All $CH_2$ wagging | 1259.7 |
| 40 | 1486.7 | 1338.4 | 1349.7 | 1347.0 | 1280.9 | 1354.4 | 1422.2 | 1297.1 | Wagging $C(2)H_2$, $C(7)H_2$; twist $C(5)H_2$, $C(10)H_2$ | 1283.6 |
| 41 | 1513.7 | 1369.3 | 1376.8 | 1375.4 | 1324.1 | 1363.1 | 1429.9 | 1310.2 | All $CH_2$ wagging | 1313.1 |
| 42 | 1526.5 | 1376.9 | 1396.5 | 1392.5 | 1331.0 | 1365.8 | 1432.3 | 1312.6 | All $CH_2$ wagging | 1320.4 |
| 43 | 1558.1 | 1427.8 | 1444.8 | 1441.9 | 1343.5 | 1375.3 | 1439.4 | 1317.6 | Wagging $C(5)H_2$, $C(10)H_2$ | 1369.2 |
| 44 | 1582.4 | 1445.3 | 1458.6 | 1457.3 | 1344.1 | 1376.5 | 1442.7 | 1318.6 | Wagging $C(5)H_2$, $C(10)H_2$ | 1386.0 |
| 45 | 1601.3 | 1467.3 | 1459.0 | 1458.9 | 1349.7 | 1470.4 | 1503.8 | 1340.4 | Scissors $C(2)H_2$, $C(7)H_2$ | 1407.2 |
| 46 | 1602.0 | 1467.6 | 1460.2 | 1459.0 | 1396.6 | 1503.0 | 1539.3 | 1381.9 | Scissors $C(2)H_2$, $C(7)H_2$ | 1407.5 |
| 47 | 1644.7 | 1518.9 | 1511.3 | 1511.4 | 1446.7 | 1627.2 | 1617.7 | 1413.4 | Scissors $C(5)H_2$, $C(10)H_2$ | 1456.6 |
| 48 | 1650.8 | 1528.4 | 1523.0 | 1522.8 | 1450.7 | 1630.8 | 1645.0 | 1437.4 | Scissors $C(5)H_2$, $C(10)H_2$ | 1465.8 |
| 49 | 1926.9 | 1721.7 | 1741.3 | 1737.0 | 1805.1 | 1835.1 | 1870.6 | 1730.1 | Stretch C=N | 1651.1 |
| 50 | 1933.4 | 1722.6 | 1742.3 | 1738.0 | 1812.2 | 1840.0 | 1874.2 | 1732.0 | Stretch C=N | 1652.0 |
| 51 | 2024.4 | 1842.7 | 1864.4 | 1860.5 | 1987.5 | 2083.4 | 2165.1 | 1941.7 | Stretch C=O | 1767.2 |
| 52 | 2027.6 | 1845.3 | 1866.9 | 1863.0 | 1991.6 | 2087.9 | 2168.6 | 1946.9 | Stretch C=O | 1769.6 |
| 53 | 3227.1 | 3036.1 | 3052.3 | 3048.0 | 2908.2 | 2950.2 | 3193.2 | 3293.1 | Stretch symmetric $C(5)H_2$, $C(10)H_2$ | 2911.6 |
| 54 | 3228.1 | 3036.2 | 3052.5 | 3048.1 | 2908.3 | 2950.4 | 3193.5 | 3294.3 | Stretch symmetric $C(5)H_2$, $C(10)H_2$ | 2911.8 |
| 55 | 3248.5 | 3072.8 | 3085.9 | 3081.5 | 2966.7 | 3015.5 | 3236.8 | 3314.0 | Stretch symmetric $C(2)H_2$, $C(7)H_2$ | 2946.8 |
| 56 | 3248.6 | 3072.8 | 3086.0 | 3081.6 | 2966.8 | 3015.6 | 3236.8 | 3315.4 | Stretch symmetric $C(2)H_2$, $C(7)H_2$ | 2946.8 |
| 57 | 3289.5 | 3108.5 | 3126.5 | 3122.4 | 2977.2 | 3022.9 | 3253.5 | 3368.2 | Stretch asymmetric $C(2)H_2$, $C(7)H_2$ | 2981.1 |
| 58 | 3289.5 | 3108.6 | 3126.6 | 3122.4 | 2977.5 | 3023.5 | 3253.7 | 3368.4 | Stretch asymmetric $C(2)H_2$, $C(7)H_2$ | 2981.1 |
| 59 | 3337.2 | 3139.8 | 3153.2 | 3150.8 | 3025.8 | 3079.7 | 3295.3 | 3378.7 | Stretch asymmetric $C(5)H_2$, $C(10)H_2$ | 3011.1 |
| 60 | 3337.6 | 3140.2 | 3153.6 | 3151.3 | 3026.1 | 3080.2 | 3295.4 | 3379.3 | Stretch asymmetric $C(5)H_2$, $C(10)H_2$ | 3011.4 |

[a] Based on B3LYP.
[b] B3LYP scaled by sf = 0.959 [20].

Table 4
Gas-phase vibration frequencies (in $cm^{-1}$) calculated directly by different methods and the corresponding scaled B3LYP values for tetrahydroimidazo[1,2-*a*]imidazo[1,2-*d*]pyrazine-3,8-dione (**4**)

| Mode | HF | B3LYP | B3P86 | B3PW91 | PM3 | AM1 | MNDO | MINDO/3 | Approximate description[a] | B3LYP scaled[b] |
|---|---|---|---|---|---|---|---|---|---|---|
| 1 | 24.0 | 35.5 | 35.2 | 35.5 | 42.1 | 21.4 | 43.6 | 51.7 | Pyrazine ring deform | 34.0 |
| 2 | 92.3 | 88.5 | 89.1 | 88.7 | 67.9 | 54.1 | 70.3 | 73.2 | Rings deform | 84.9 |
| 3 | 141.5 | 148.5 | 152.9 | 153.7 | 133.1 | 78.4 | 121.8 | 140.9 | Pyrazine ring deform | 142.4 |
| 4 | 169.9 | 171.6 | 173.0 | 172.8 | 182.7 | 150.0 | 146.3 | 208.3 | Rings deform | 164.5 |
| 5 | 230.5 | 209.0 | 209.4 | 209.5 | 209.7 | 225.5 | 235.3 | 218.5 | C=O deform in-plane | 200.5 |
| 6 | 263.8 | 243.6 | 243.7 | 243.6 | 227.3 | 239.8 | 237.2 | 227.1 | Rock $CH_2$ | 233.6 |
| 7 | 275.4 | 251.3 | 250.3 | 250.7 | 246.0 | 261.9 | 248.3 | 254.5 | C=O deform in-plane | 241.0 |
| 8 | 292.0 | 279.0 | 280.5 | 280.2 | 261.9 | 279.6 | 294.1 | 258.4 | Rings deform | 267.6 |
| 9 | 470.4 | 439.2 | 441.9 | 441.0 | 359.0 | 384.9 | 367.9 | 362.0 | Pyrazine ring deform | 421.2 |
| 10 | 495.0 | 458.5 | 461.2 | 460.3 | 421.7 | 471.5 | 447.0 | 396.1 | Rings deform | 439.7 |
| 11 | 556.2 | 515.6 | 518.4 | 518.4 | 481.9 | 522.8 | 538.6 | 467.2 | C(2)H, C(3)=O deform in-plane | 494.5 |
| 12 | 572.9 | 519.1 | 518.9 | 518.7 | 509.7 | 524.3 | 541.5 | 476.9 | Rock $CH_2$ | 497.8 |
| 13 | 577.8 | 528.3 | 532.0 | 531.7 | 522.8 | 554.4 | 548.5 | 477.5 | Rock $CH_2$ | 506.7 |
| 14 | 689.4 | 636.5 | 640.4 | 639.8 | 558.4 | 580.8 | 574.8 | 514.5 | Rock $CH_2$ | 610.4 |
| 15 | 690.8 | 639.5 | 644.7 | 643.7 | 580.4 | 615.4 | 608.4 | 552.2 | Rings deform | 613.3 |
| 16 | 700.6 | 641.1 | 645.0 | 644.0 | 598.1 | 675.3 | 640.7 | 556.6 | Rings deform | 614.9 |
| 17 | 729.4 | 674.7 | 679.2 | 677.9 | 636.9 | 699.3 | 667.8 | 577.6 | Rings deform | 647.0 |
| 18 | 786.4 | 731.6 | 734.4 | 732.9 | 663.6 | 705.7 | 696.0 | 604.1 | Rings deform | 701.6 |
| 19 | 798.4 | 737.4 | 740.3 | 739.6 | 700.0 | 770.2 | 732.4 | 624.9 | Rings deform | 707.2 |
| 20 | 813.1 | 744.2 | 754.6 | 752.8 | 741.2 | 824.7 | 785.6 | 646.2 | Breath rings | 713.7 |
| 21 | 874.4 | 806.1 | 811.3 | 809.3 | 804.9 | 883.2 | 887.5 | 755.3 | Rings deform | 773.0 |
| 22 | 890.6 | 830.3 | 837.2 | 836.0 | 871.2 | 893.9 | 935.8 | 779.7 | Rings deform | 796.2 |
| 23 | 964.6 | 835.7 | 838.6 | 837.0 | 884.8 | 931.2 | 982.1 | 816.7 | C(10)H deform out-of plane | 801.4 |
| 24 | 1031.6 | 898.0 | 899.4 | 899.0 | 896.8 | 974.5 | 986.4 | 863.3 | C(2)H deform out-of-plane | 861.2 |
| 25 | 1082.5 | 983.6 | 979.6 | 979.2 | 903.4 | 988.8 | 1028.9 | 875.8 | Rock C(7)$H_2$ | 943.3 |
| 26 | 1095.0 | 987.7 | 1001.6 | 999.3 | 909.9 | 993.4 | 1032.5 | 918.2 | CH deform in-plane; wagging C(7)$H_2$ | 947.2 |
| 27 | 1119.2 | 1016.2 | 1011.5 | 1011.2 | 977.1 | 1074.0 | 1115.7 | 995.8 | Rock C(5)$H_2$ | 974.6 |
| 28 | 1142.0 | 1042.7 | 1064.7 | 1062.2 | 998.6 | 1074.2 | 1154.6 | 1014.0 | CH deform in-plane; wagging C(5)$H_2$; stretch C(7)N | 999.9 |
| 29 | 1175.7 | 1083.1 | 1092.4 | 1090.7 | 1023.9 | 1104.3 | 1166.9 | 1014.3 | CH deform in-plane | 1038.6 |
| 30 | 1237.8 | 1128.0 | 1147.9 | 1143.5 | 1041.6 | 1158.4 | 1236.3 | 1086.6 | C(3)=O deform in-plane | 1081.8 |
| 31 | 1274.9 | 1180.1 | 1193.9 | 1190.8 | 1052.1 | 1169.6 | 1247.9 | 1111.8 | Rings deform | 1131.7 |
| 32 | 1307.2 | 1189.3 | 1196.1 | 1196.4 | 1118.5 | 1193.7 | 1254.0 | 1141.3 | Wagging $CH_2$; CH deform in-plane | 1140.5 |
| 33 | 1319.5 | 1195.5 | 1202.9 | 1200.5 | 1125.5 | 1251.5 | 1269.1 | 1156.1 | Twist C(7)$H_2$ | 1146.4 |
| 34 | 1357.2 | 1240.9 | 1240.6 | 1242.1 | 1144.6 | 1270.8 | 1333.4 | 1175.3 | Twist C(5)$H_2$ | 1190.0 |
| 35 | 1374.9 | 1247.6 | 1254.4 | 1253.3 | 1177.4 | 1309.8 | 1350.2 | 1191.6 | Wagging $CH_2$; CH deform in-plane | 1196.5 |
| 36 | 1434.2 | 1301.0 | 1301.6 | 1301.5 | 1238.8 | 1327.9 | 1396.5 | 1273.7 | Wagging $CH_2$; C(10)H deform in-plane | 1247.6 |
| 37 | 1457.7 | 1327.1 | 1336.0 | 1333.9 | 1275.0 | 1346.3 | 1420.2 | 1276.8 | C(2)H deform in-plane | 1272.7 |
| 38 | 1505.4 | 1355.4 | 1370.9 | 1368.1 | 1324.4 | 1365.2 | 1435.5 | 1308.3 | Wagging $CH_2$; C(10)H deform in-plane | 1299.9 |
| 39 | 1525.8 | 1384.0 | 1393.2 | 1391.4 | 1335.9 | 1375.4 | 1436.6 | 1312.0 | Wagging $CH_2$ | 1327.2 |
| 40 | 1548.3 | 1424.4 | 1447.2 | 1443.2 | 1342.1 | 1450.9 | 1507.1 | 1330.2 | Stretch C(10)N | 1366.0 |
| 41 | 1584.2 | 1449.6 | 1461.9 | 1461.5 | 1381.2 | 1466.3 | 1526.1 | 1341.6 | Wagging C(5)$H_2$; C(10)H deform in-plane | 1390.2 |
| 42 | 1603.1 | 1470.2 | 1468.4 | 1465.5 | 1407.6 | 1626.7 | 1596.4 | 1400.5 | Scissors C(7)$H_2$ | 1409.9 |
| 43 | 1651.6 | 1528.5 | 1522.9 | 1522.5 | 1450.7 | 1654.8 | 1633.1 | 1427.8 | Scissors C(5)$H_2$ | 1465.8 |
| 44 | 1814.6 | 1569.2 | 1585.9 | 1583.7 | 1761.8 | 1785.2 | 1804.1 | 1675.1 | Stretch C(2)=N | 1504.9 |
| 45 | 1926.2 | 1720.7 | 1739.3 | 1734.9 | 1814.4 | 1843.6 | 1865.6 | 1734.6 | Stretch C(5a)=N | 1650.1 |
| 46 | 1947.8 | 1741.2 | 1758.5 | 1754.0 | 1865.5 | 1870.9 | 1879.4 | 1792.1 | Stretch C=C | 1669.8 |
| 47 | 2009.6 | 1809.3 | 1831.5 | 1827.5 | 1983.4 | 2077.9 | 2157.9 | 1923.4 | Stretch C(3)=O | 1735.2 |
| 48 | 2035.9 | 1852.0 | 1873.9 | 1870.0 | 1994.0 | 2093.2 | 2173.2 | 1947.2 | Stretch C(8)=O | 1776.1 |
| 49 | 3250.6 | 3063.2 | 3076.5 | 3072.4 | 2909.8 | 2945.8 | 3192.0 | 3285.2 | Stretch symmetric C(5)$H_2$ | 2937.6 |
| 50 | 3257.1 | 3074.9 | 3087.7 | 3083.4 | 2965.3 | 3012.0 | 3236.6 | 3309.0 | Stretch symmetric C(7)$H_2$ | 2948.8 |
| 51 | 3292.1 | 3094.3 | 3112.7 | 3109.3 | 2979.6 | 3018.0 | 3251.9 | 3368.7 | Stretch asymmetric C(5)$H_2$ | 2967.4 |
| 52 | 3300.4 | 3110.0 | 3127.6 | 3123.6 | 3024.4 | 3076.5 | 3294.7 | 3379.3 | Stretch asymmetric C(7)$H_2$ | 2982.5 |
| 53 | 3428.8 | 3245.3 | 3260.5 | 3256.0 | 3029.7 | 3145.1 | 3409.4 | 3451.1 | Stretch C(2)H | 3112.2 |
| 54 | 3472.4 | 3282.1 | 3292.9 | 3290.1 | 3080.3 | 3203.7 | 3438.5 | 3461.9 | Stretch C(10)H | 3147.6 |

[a] Based on B3LYP.
[b] B3LYP scaled by sf = 0.959 [20].

Table 5
Gas-phase vibration frequencies (in $cm^{-1}$) calculated directly by different methods and the corresponding scaled B3LYP values for dihydroimidazo[1,2-*a*]imidazo[1,2-*d*]pyrazine-3,8-dione (**5**)

| Mode | HF | B3LYP | B3P86 | B3PW91 | PM3 | AM1 | MNDO | MINDO/3 | Approximate description[a] | B3LYP scaled[b] |
|---|---|---|---|---|---|---|---|---|---|---|
| 1 | 82.3 | 84.0 | 84.2 | 84.1 | 68.6 | 70.8 | 66.8 | 59.5 | Rings deform | 80.6 |
| 2 | 123.5 | 122.4 | 123.3 | 123.3 | 93.0 | 87.6 | 96.1 | 110.5 | Rings deform | 117.3 |
| 3 | 177.4 | 195.8 | 197.9 | 197.3 | 144.9 | 135.7 | 142.4 | 144.7 | Rings deform | 187.8 |
| 4 | 234.3 | 212.4 | 212.7 | 212.8 | 213.9 | 214.5 | 212.8 | 209.1 | Imidazole ring deform | 203.7 |
| 5 | 281.2 | 254.4 | 253.4 | 253.9 | 223.0 | 230.1 | 238.7 | 213.7 | Pyrazine ring deform; C=O deform in-plane | 244.0 |
| 6 | 285.2 | 270.0 | 271.1 | 270.6 | 240.6 | 259.2 | 248.2 | 256.1 | Rings deform | 259.0 |
| 7 | 293.1 | 292.6 | 293.9 | 293.8 | 269.1 | 285.9 | 298.6 | 277.7 | Rings deform | 280.6 |
| 8 | 479.0 | 437.7 | 439.8 | 438.8 | 354.9 | 372.3 | 359.0 | 342.3 | Rings deform | 419.8 |
| 9 | 490.6 | 464.1 | 466.2 | 465.3 | 382.7 | 401.0 | 381.4 | 370.8 | Rings deform | 445.1 |
| 10 | 499.2 | 465.1 | 467.3 | 466.5 | 438.2 | 489.1 | 469.9 | 413.1 | Pyrazine ring deform | 446.0 |
| 11 | 575.0 | 533.0 | 536.0 | 535.8 | 486.2 | 531.2 | 544.1 | 472.6 | C=O deform in-plane | 511.1 |
| 12 | 578.5 | 539.2 | 541.9 | 541.5 | 523.9 | 566.9 | 554.3 | 475.1 | Pyrazine ring deform | 517.1 |
| 13 | 686.5 | 645.5 | 649.6 | 648.5 | 566.9 | 598.9 | 588.1 | 517.9 | Rings deform | 619.0 |
| 14 | 719.0 | 667.2 | 670.9 | 670.0 | 581.0 | 608.2 | 590.1 | 547.3 | Imidazole ring deform | 639.8 |
| 15 | 723.5 | 668.2 | 673.0 | 671.5 | 598.1 | 682.9 | 654.5 | 561.8 | Rings deform | 640.8 |
| 16 | 727.6 | 675.4 | 679.9 | 679.0 | 643.5 | 695.1 | 681.2 | 583.2 | Rings deform | 647.7 |
| 17 | 802.6 | 725.9 | 728.6 | 727.9 | 661.8 | 702.8 | 693.0 | 612.2 | Rings deform | 696.1 |
| 18 | 806.8 | 726.0 | 729.1 | 728.3 | 664.8 | 713.9 | 695.8 | 612.7 | Rings deform | 696.2 |
| 19 | 808.1 | 759.8 | 765.9 | 764.1 | 730.9 | 800.8 | 762.5 | 630.1 | Rings deform | 728.7 |
| 20 | 845.3 | 786.6 | 791.8 | 790.2 | 745.1 | 833.2 | 792.7 | 646.1 | Rings deform | 754.4 |
| 21 | 862.5 | 801.2 | 807.8 | 805.7 | 830.3 | 903.2 | 911.4 | 764.6 | Rings deform | 768.3 |
| 22 | 914.1 | 853.6 | 861.5 | 860.1 | 886.5 | 903.7 | 954.5 | 772.4 | Breath imidazole ring; C(5)H, C(10)H deform in-plane | 818.6 |
| 23 | 984.7 | 877.6 | 879.5 | 878.8 | 887.8 | 922.1 | 956.9 | 779.5 | All CH deform out-of-plane | 841.7 |
| 24 | 990.0 | 879.8 | 881.0 | 880.4 | 892.4 | 922.2 | 978.7 | 779.9 | All CH deform out-of-plane | 843.7 |
| 25 | 1030.7 | 897.6 | 899.2 | 898.6 | 903.2 | 925.7 | 982.5 | 833.5 | All CH deform out-of-plane | 860.8 |
| 26 | 1032.9 | 902.8 | 905.0 | 904.4 | 912.2 | 993.6 | 1009.8 | 937.4 | All CH deform out-of-plane | 865.8 |
| 27 | 1125.9 | 1027.6 | 1040.1 | 1037.4 | 1005.5 | 1087.0 | 1141.9 | 1006.4 | Pyrazine ring deform; C(2)H, C(7)H deform in-plane | 985.5 |
| 28 | 1158.2 | 1060.0 | 1070.4 | 1069.3 | 1025.3 | 1103.0 | 1173.8 | 1016.1 | C(5)H, C(10)H deform in-plane | 1016.6 |
| 29 | 1271.6 | 1135.7 | 1153.2 | 1149.1 | 1086.4 | 1153.3 | 1243.9 | 1096.7 | Stretch C(=O)C | 1089.1 |
| 30 | 1271.8 | 1149.8 | 1165.2 | 1162.4 | 1118.1 | 1178.4 | 1255.5 | 1156.0 | C(2)H, C(7)H deform in-plane | 1102.7 |
| 31 | 1327.9 | 1227.3 | 1237.3 | 1235.0 | 1152.8 | 1244.8 | 1301.6 | 1175.7 | Pyrazine ring deform; C(2)H, C(7)H deform in-plane | 1177.0 |
| 32 | 1361.0 | 1236.1 | 1237.9 | 1238.0 | 1181.8 | 1275.9 | 1329.0 | 1177.5 | All CH deform in-plane | 1185.4 |
| 33 | 1382.2 | 1269.3 | 1274.6 | 1273.6 | 1189.7 | 1297.1 | 1353.1 | 1195.9 | All CH deform in-plane | 1217.3 |
| 34 | 1442.9 | 1330.2 | 1337.8 | 1336.1 | 1221.2 | 1350.6 | 1404.1 | 1260.6 | C(2)H, C(7)H deform in-plane | 1275.7 |
| 35 | 1471.8 | 1339.9 | 1358.8 | 1355.8 | 1318.6 | 1411.5 | 1496.0 | 1283.1 | C(2)H, C(7)H deform in-plane | 1285.0 |
| 36 | 1512.9 | 1374.9 | 1382.1 | 1381.5 | 1349.5 | 1421.2 | 1496.5 | 1300.6 | C(5)H, C(10)H deform in-plane | 1318.5 |
| 37 | 1513.4 | 1398.7 | 1424.0 | 1419.4 | 1399.5 | 1619.6 | 1570.0 | 1392.7 | Stretch C—N | 1341.3 |
| 38 | 1596.3 | 1456.8 | 1480.6 | 1475.8 | 1434.3 | 1668.3 | 1634.3 | 1426.7 | Stretch C—N | 1397.0 |
| 39 | 1795.4 | 1531.8 | 1548.6 | 1546.1 | 1742.9 | 1749.2 | 1774.4 | 1651.6 | Stretch C=N | 1469.0 |
| 40 | 1798.1 | 1543.3 | 1561.2 | 1558.8 | 1744.0 | 1753.1 | 1778.3 | 1653.5 | Stretch C=N | 1480.0 |
| 41 | 1893.6 | 1682.7 | 1700.3 | 1696.0 | 1841.6 | 1842.2 | 1843.8 | 1773.6 | Stretch C=C | 1613.7 |
| 42 | 1952.0 | 1742.6 | 1759.5 | 1755.2 | 1856.6 | 1850.2 | 1848.2 | 1773.9 | Stretch C=C | 1671.1 |
| 43 | 1994.1 | 1800.1 | 1822.5 | 1818.7 | 1974.5 | 2069.7 | 2152.0 | 1904.1 | Stretch C=O | 1726.3 |
| 44 | 2025.0 | 1816.3 | 1839.0 | 1835.0 | 1992.8 | 2093.8 | 2171.2 | 1937.5 | Stretch C=O | 1741.8 |
| 45 | 3432.0 | 3252.7 | 3267.3 | 3262.5 | 3026.2 | 3133.7 | 3403.3 | 3444.0 | Stretch C(2)H, C(7)H | 3119.3 |
| 46 | 3432.0 | 3253.0 | 3268.1 | 3263.1 | 3027.0 | 3133.9 | 3403.5 | 3445.8 | Stretch C(2)H, C(7)H | 3119.6 |
| 47 | 3466.4 | 3271.0 | 3281.9 | 3279.0 | 3078.0 | 3202.3 | 3438.8 | 3463.8 | Stretch C(5)H, C(10)H | 3136.9 |
| 48 | 3467.1 | 3271.3 | 3282.1 | 3279.1 | 3078.4 | 3203.0 | 3438.9 | 3464.1 | Stretch C(5)H, C(10)H | 3137.2 |

[a] Based on B3LYP.
[b] B3LYP scaled by sf = 0.959 [20].

B3PW91 methods and 6-31G(*d*) basis set. The HyperChem Version 5.1 package was used for the semi-empirical calculations (Polak–Ribiere conjugate gradient algorithm, convergence limit of 0.001 kcal $mol^{-1}$, root mean square gradient of 0.001 kcal $Å^{-1}$ $mol^{-1}$) and normal mode visualization.

## 3. Results and discussion

Vibration frequencies calculated by different semi-empirical (PM3, AM1, MNDO and MINDO/3), HF, and hybrid DFT (B3LYP, B3P86 and B3PW91) methods for the glycine derivatives **1**–**5** are listed in Tables 1–5, with the corresponding theoretical IR spectra presented in Figs. 2–6, respectively. Semi-empirical methods do not have sufficient performance to make direct prediction of experimental gas-phase spectra for the class of compounds of interest [18]. Nevertheless, their comparison to more precise methods can be useful in the future to treat more extended molecular systems of similar chemical nature, where ab initio and DFT calculations might have a prohibitive cost.

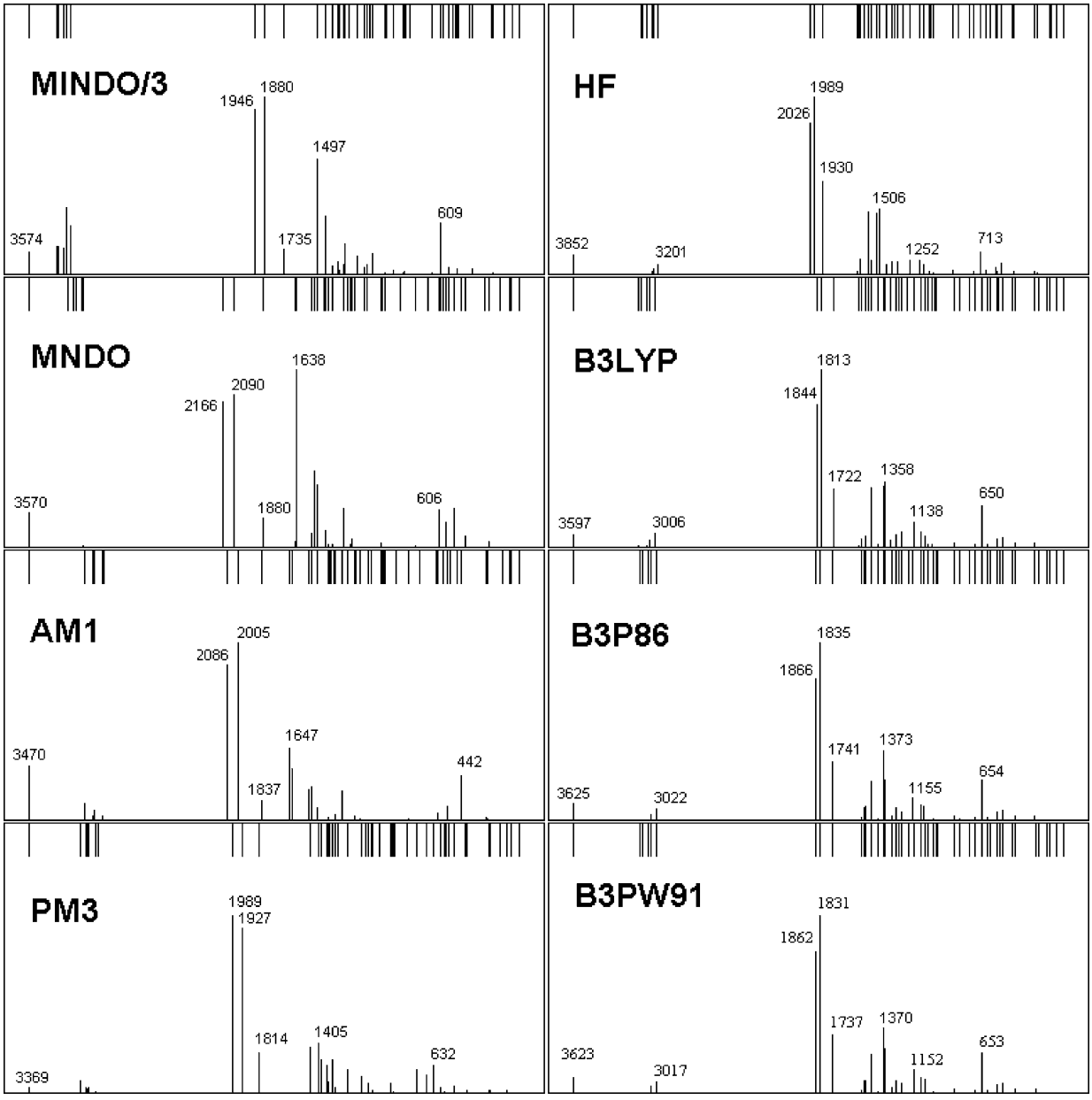


Fig. 2. IR spectra of hexahydroimidazo[1,2-*a*]pyrazine-3,6-dione (**1**) calculated by different methods. Top bars represent all fundamental frequencies; bottom bars, IR-active vibrations; wavenumbers in $cm^{-1}$.

As we found earlier [19,20], HF method is much more precise, with a coefficient for correlation between the calculated and experimental wavenumbers of 0.9992–0.9995. The latter further increases for the hybrid DFT methods, approaching values of 0.9999. In principle, any of them (B3LYP, B3P86 and B3PW91) can be almost equally used for the IR spectral predictions. However B3LYP produces less overestimated values for wavenumbers and requires applying the highest scaling factor of 0.959 as compared to the other two hybrid functionals (0.954 and 0.955 for B3P86 and B3PW91, respectively). That is why we base our predictions upon the B3LYP data, by correcting the calculated wavenumbers by a factor of 0.959 (last columns in Tables 1–5).

The most important characteristic absorption bands correspond to stretching vibrations involving the N and O heteroatoms. The highest frequency band would be found in the spectra of **1** and **2** due to $\nu_{NH}$, at 3450.4 and 3462.1 $cm^{-1}$ (scaled values), respectively. For the same compounds, three most intense bands are observed in the region of C=C, C=N and C=O vibrations at 1650–1800 $cm^{-1}$. For more symmetric molecules **3** and **5**, due to the presence of equivalent bonds, one can see only two such bands here. The C=N stretching modes deserve special attention. Two types of chemical environment involving C=N bonds can be distinguished in **1**–**5**. In **2**, **4** and **5**, where C=N bonds are conjugated with C=O and C=C bonds, one can observe medium-intensity bands

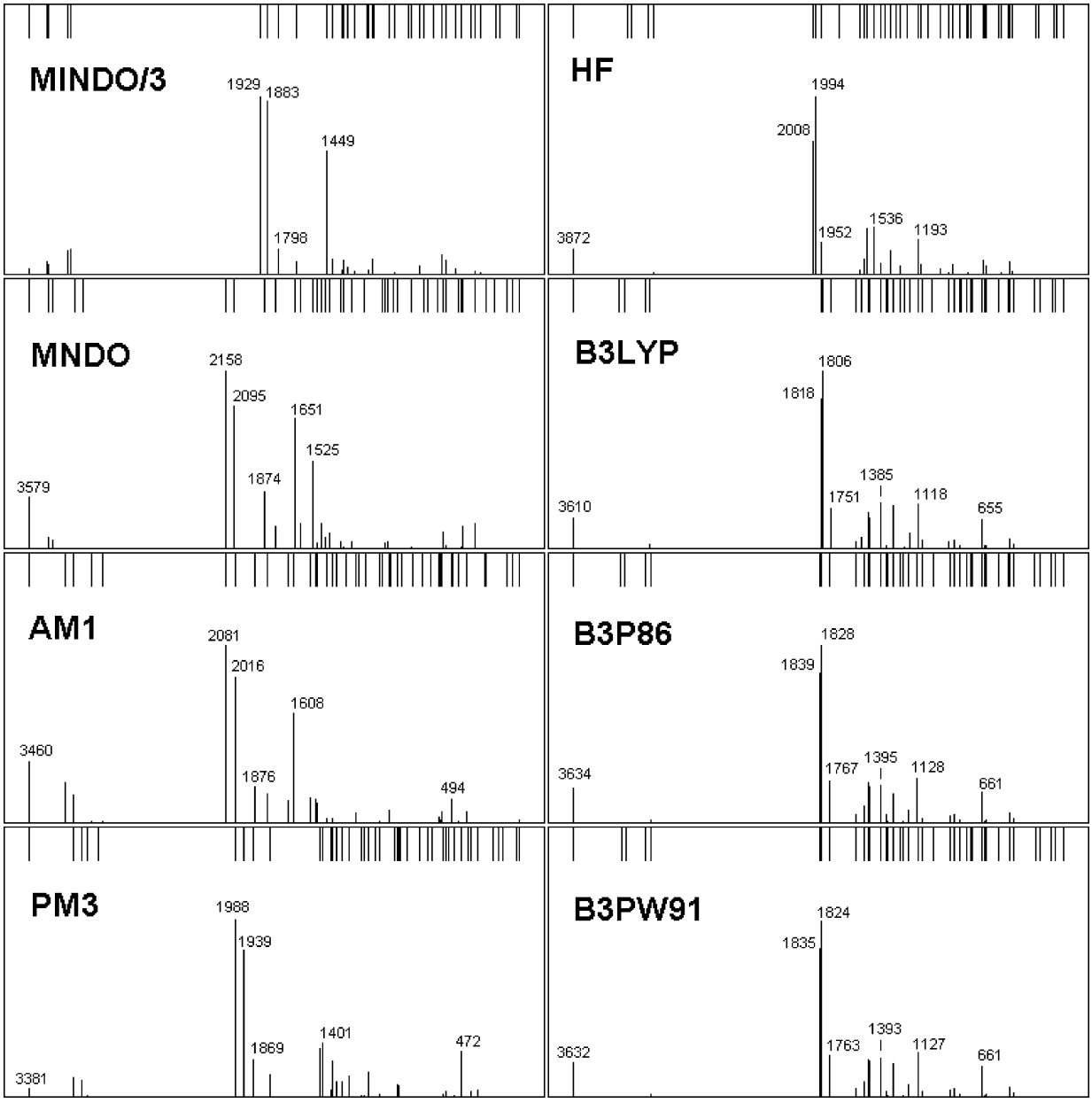


Fig. 3. IR spectra of tetrahydroimidazo[1,2-*a*]pyrazine-3,6-dione (**2**) calculated by different methods. Top bars represent all fundamental frequencies; bottom bars, IR-active vibrations; wavenumbers in $cm^{-1}$.

at ca. 1500 $cm^{-1}$ or lower frequency. At the same time, for C(8a) = N and C(5a) = N in **1** and **3**, respectively, the frequencies are as high as ca. 1652 $cm^{-1}$, approaching values more typical for double bonds. In **4**, both C=N bond and corresponding absorption band types are present. Another interesting feature of its IR spectrum is a very intense band at ca. 1424 $cm^{-1}$, B3LYP unscaled (Fig. 5), which can be expected at 1366 $cm^{-1}$ in the experimental spectrum. It was attributed to C(10)–N stretching vibrations, and has an absolute intensity of 546 km $mol^{-1}$, much higher than those for similar bands in any other amidine molecule.

Despite molecule **2** has four double bonds, only three $\nu_{C=X}$ bands can be distinguished in its calculated IR spectrum (Fig. 3), $\nu_{C(6)=O}$ at 1818, $\nu_{C(3)=O}$ at 1806 and $\nu_{C=C}$ at 1751 $cm^{-1}$ (B3LYP unscaled). The fourth band of $\nu_{C(2)=N}$ (mode 34; Table 2) has a very low intensity of 24 km $mol^{-1}$ and cannot be noticed. The C=O bands for **2** are much closer to each other as compared to the case of molecule **1** (12 cm and 30 $cm^{-1}$, respectively). This is evidently an effect of conjugation with C=N and C=C bonds in dehydrogenated amidine **2**. On the other hand, the predicted interval between $\nu_{C(3)=O}$ and $\nu_{C=C}$ absorption maxima is almost 53 $cm^{-1}$, whereas in the case of analogous alanine derivative it was 23 $cm^{-1}$ only [20]. Thus one can expect that even common commercial FTIR detectors for gas chromatography, having resolution of

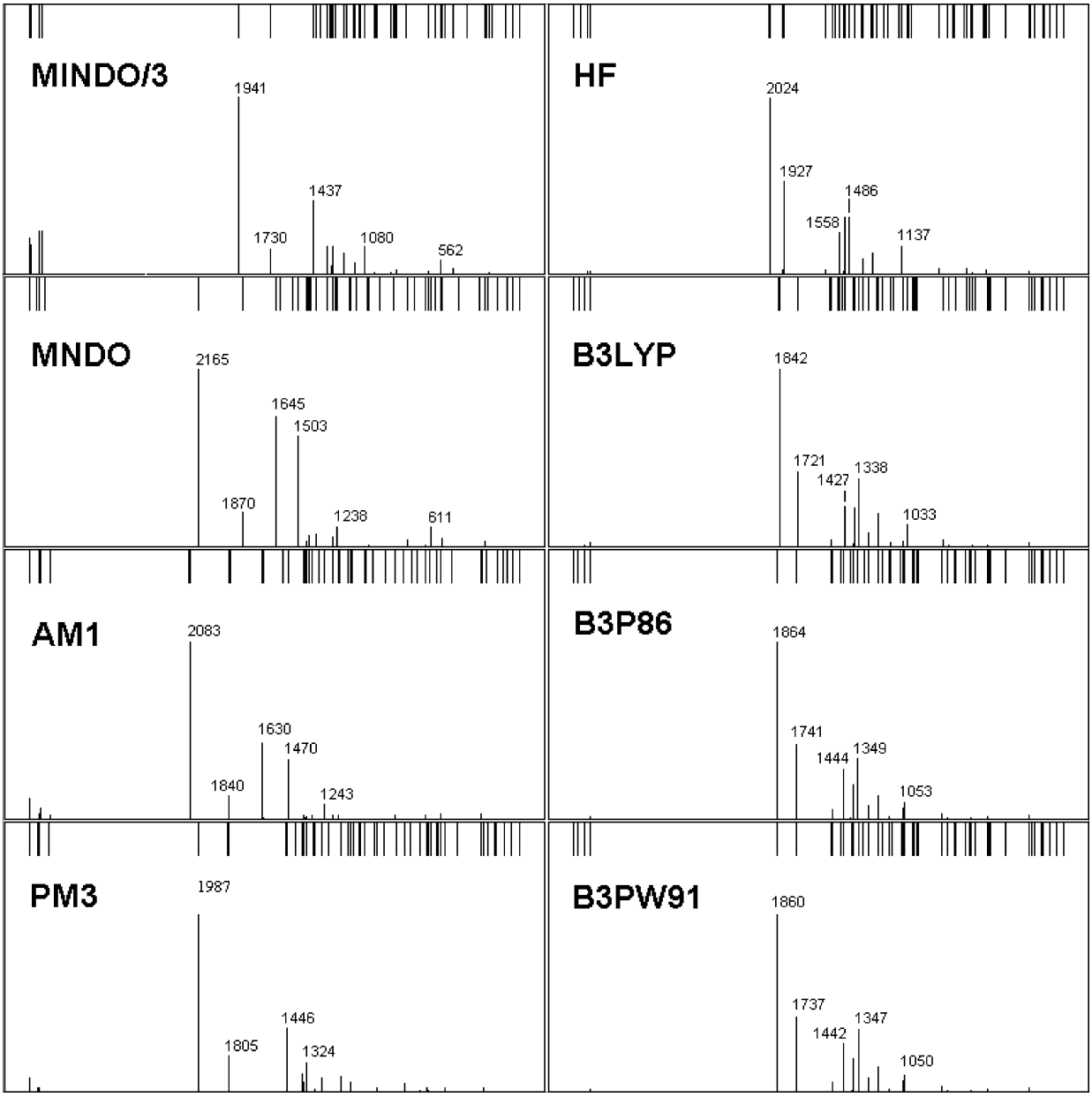


Fig. 4. IR spectra of hexahydroimidazo[1,2-*a*]imidazo[1,2-*d*]pyrazine-3,8-dione (**3**) calculated by different methods. Top bars represent all fundamental frequencies; bottom bars, IR-active vibrations; wavenumbers in $cm^{-1}$.

4–8 $cm^{-1}$, would be able to separate the C=C band from the two unresolved carbonyl bands, contrary to the case of alanine.

As it was already mentioned, there are two equivalent C=O and two equivalent C=N bonds in tricyclic amidine **3**, producing only two visible and intense bands in the region of $\nu_{C=X}$ vibrations (Fig. 4). Nevertheless, four modes 49–52 are IR-active, as can be seen from Table 3. The carbonyl band intensities are 635 (mode 51) and 4 km $mol^{-1}$ (mode 52), for C=N bands they are 273 (mode 49) and 17 km $mol^{-1}$ (mode 50), with shifts of 2.4 and 0.9 $cm^{-1}$ for the scaled wavenumbers, respectively. A very similar situation can be observed for doubly dehydrogenated amidine **5** (Fig. 6; Table 5), where three bands only are visible the region of $\nu_{C=X}$ vibrations of six bands calculated (modes 39–44). In particular, two C=O bands with scaled frequencies of 1741.8 and 1726.3 $cm^{-1}$ have absolute intensities of 0.0008 and 1325 km $mol^{-1}$, respectively. Two C=C bands with scaled frequencies of 1671.1 and 1613.7 $cm^{-1}$ have absolute intensities of 0.0029 and 201 km $mol^{-1}$, respectively. And finally two C=N bands with scaled frequencies of 1480.0 and 1469.0 $cm^{-1}$ have absolute intensities of 0.0003 and 176 km $mol^{-1}$, respectively.

A point of special interest is behavior of the principal characteristic absorption bands, which correspond to stretching vibrations involving the N and O atoms, in comparison to IR spectra of the known related amidines. For the parent

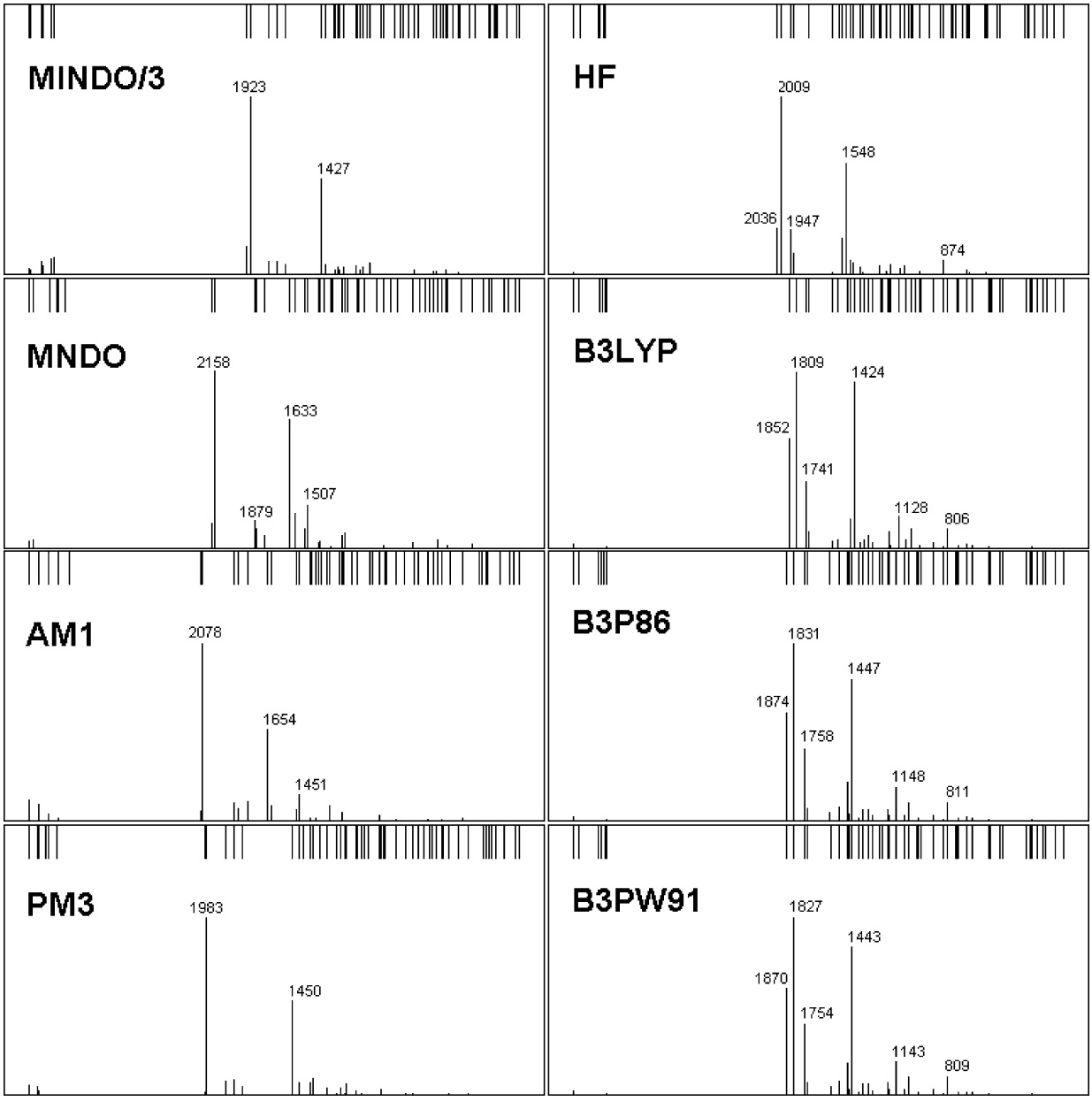


Fig. 5. IR spectra of tetrahydroimidazo[1,2-*a*]imidazo[1,2-*d*]pyrazine-3,8-dione (**4**) calculated by different methods. Top bars represent all fundamental frequencies; bottom bars, IR-active vibrations; wavenumbers in $cm^{-1}$.

bicyclic amidine **1**, two homologues have been spectrally characterized previously, the ones derived from alanine and α-aminoisobutyric acid [19,20]. The alanine derivative has three methyl substituents, whereas the α-aminoisobutyric acid derivative has as much as six such substituents. This structural difference allows us analyzing the substituent effect on IR absorption maxima. One can see that the following three important bands undergo a well-pronounced low-frequency shift in the series of Gly(B3LYP scaled)–Ala–Aib:

- $\nu_{C=N}$ 1651.8 > 1646 > 1640 $cm^{-1}$;
- $\nu_{C(3)=O}$ 1768.6 > 1762 > 1753 $cm^{-1}$;
- $\nu_{NH}$ 3450.4 > 3423 > 3402 $cm^{-1}$.

For the C(6)=O stretching band such a trend was not observed, where the corresponding wavenumbers are 1739.4, 1725 and 1730 $cm^{-1}$. However, for the parent tricyclic amidines, **3** and its homologues [14,20], in the series of Gly(B3LYP scaled)–Ala–Aib one can see it again for two most important bands:

- $\nu_{C=N}$ 1651.1 > 1646 > 1632 $cm^{-1}$;
- $\nu_{C=O}$ 1767.2 > 1758 > 1754 $cm^{-1}$.

The spectra calculated by computationally less expensive HF method generally keep most important features observed in its DFT counterparts, although HF wavenumbers are overestimated to a greater scale due to a neglect of electron cor-

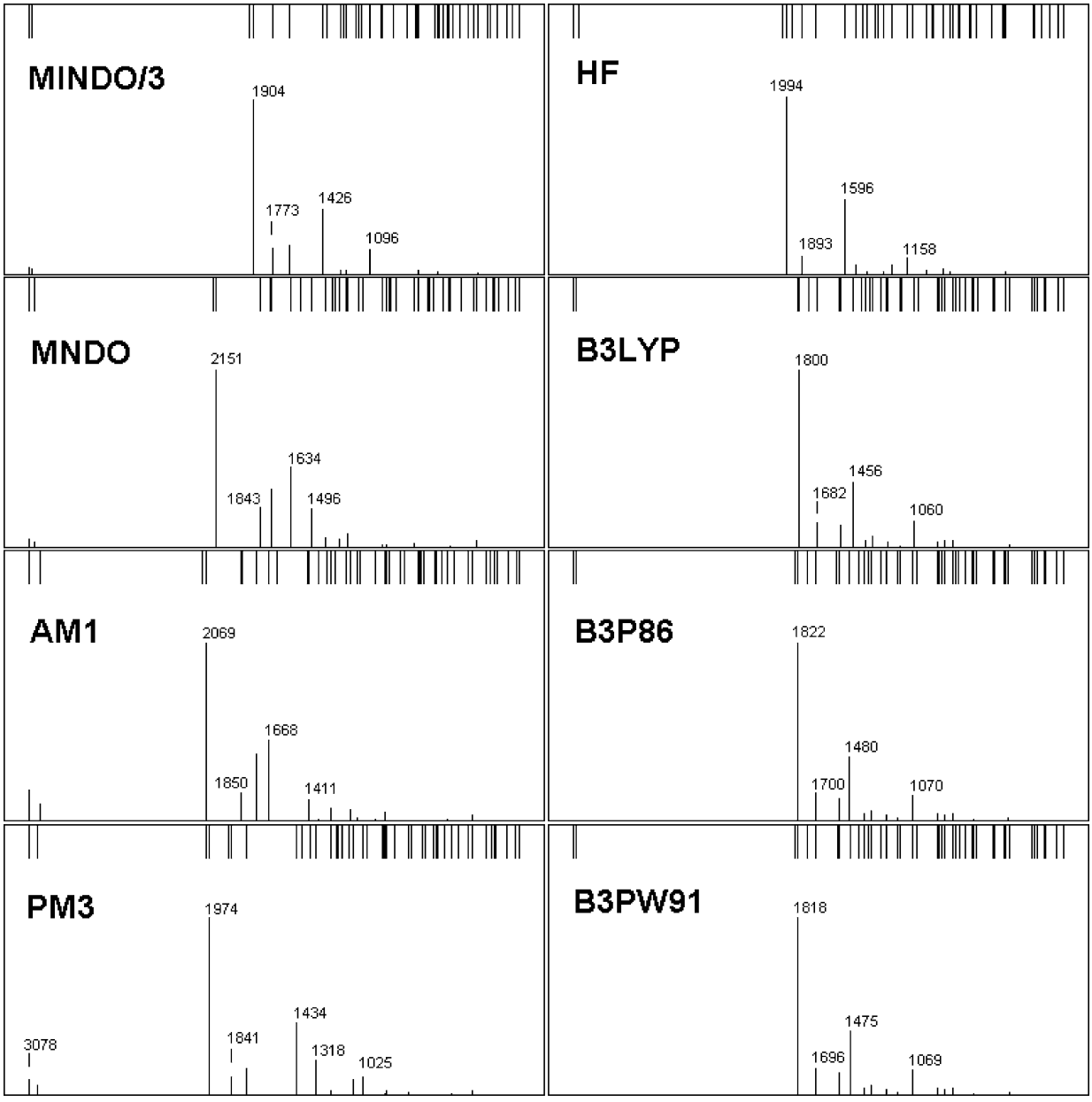


Fig. 6. IR spectra of dihydroimidazo[1,2-*a*]imidazo[1,2-*d*]pyrazine-3,8-dione (**5**) calculated by different methods. Top bars represent all fundamental frequencies; bottom bars, IR-active vibrations; wavenumbers in $cm^{-1}$.

relation. For example, an overestimation of about 250 $cm^{-1}$ exist for $\nu_{C=N}$ and $\delta_{NH}$ modes. Also, a common feature for all the HF spectra is that C=N bands for **1** and **3**, as well as C=C bands for **2**, **4** and **5** are closer to C=O bands, as compared to those in DFT-calculated spectra.

The considerations of cost-efficiency change from important to crucial when the size of molecular systems drastically increases. A good example of the systems difficult for direct high-level calculations is amidation reactions at carboxylated carbon nanotube tips (see [28–30] and references therein). Until now there is much controversy on the chemical structure of oxidized defect sites and on interpretation of the IR spectra measured. Theoretical calculations would be of great help, and semi-empirical methods could provide first preliminary data. Bearing the above in mind, we tested the performance of several semi-empirical methods, comparing the spectra calculated to the B3LYP data. A general revision reveals that PM3 produces best results in terms of visual similarity to the spectra calculated by DFT methods. Analysis of interrelations between the wavenumbers calculated by B3LYP and those calculated by other methods (Fig. 7) shows that all semi-empirical methods tend to overestimate frequencies in the most important region of $\nu_{C=X}$ vibrations (central parts of the plots). The best method in this regard is MINDO/3. On the contrary, wavenumbers in the high-frequency region often turn to be underestimated, especially

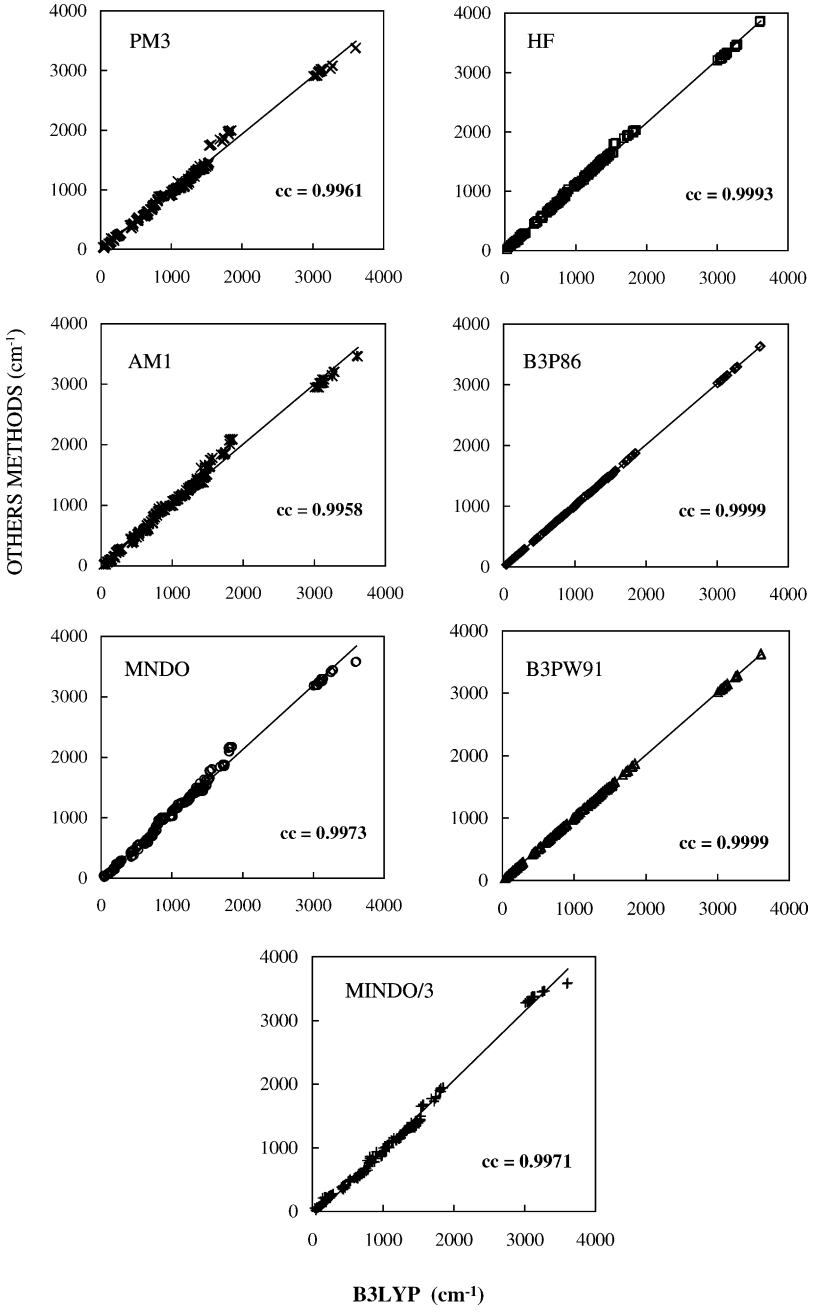


Fig. 7. Interrelation between wavenumbers calculated by B3LYP and those calculated by other methods (cc, correlation coefficient). Plots include the data for all amidines **1**–**5**.

for $\nu_{NH}$ modes. Evaluation in terms of correlation coefficients between wavenumbers calculated by B3LYP and those calculated by other methods (Fig. 7) makes us conclude that two best semi-empirical methods are MNDO (cc = 0.9973) and MINDO/3 (cc = 0.9971). In turn for the latter, the behavior of frequencies in the most important region of $\nu_{C=X}$ vibrations is somewhat more uniform that for MNDO, biasing our choice to MINDO/3.

The same central part around 1600–2000 $cm^{-1}$ is the region where HF method presents similar imperfections against B3LYP. The corresponding cc value of 0.9993 is only insignificantly lower as compared to those calculated for the hybrid DFT methods (cc = 0.9999). However the importance of $\nu_{C=X}$ bands, on one hand, and insignificantly higher computational cost of B3P86 and B3PW91, on the other hand, makes all the hybrid DFT methods tested an obvious choice for IR spectral predictions for the cyclic amidine compounds.

The last point of interest for us was a basis set effect on the B3LYP vibration frequencies, which is important to know for minimizing computation costs. Fundamental vibration frequencies were recalculated for bicyclic amidine **1**, by varying Pople basis sets from minimal STO-3G to 6-311++G(*d*,

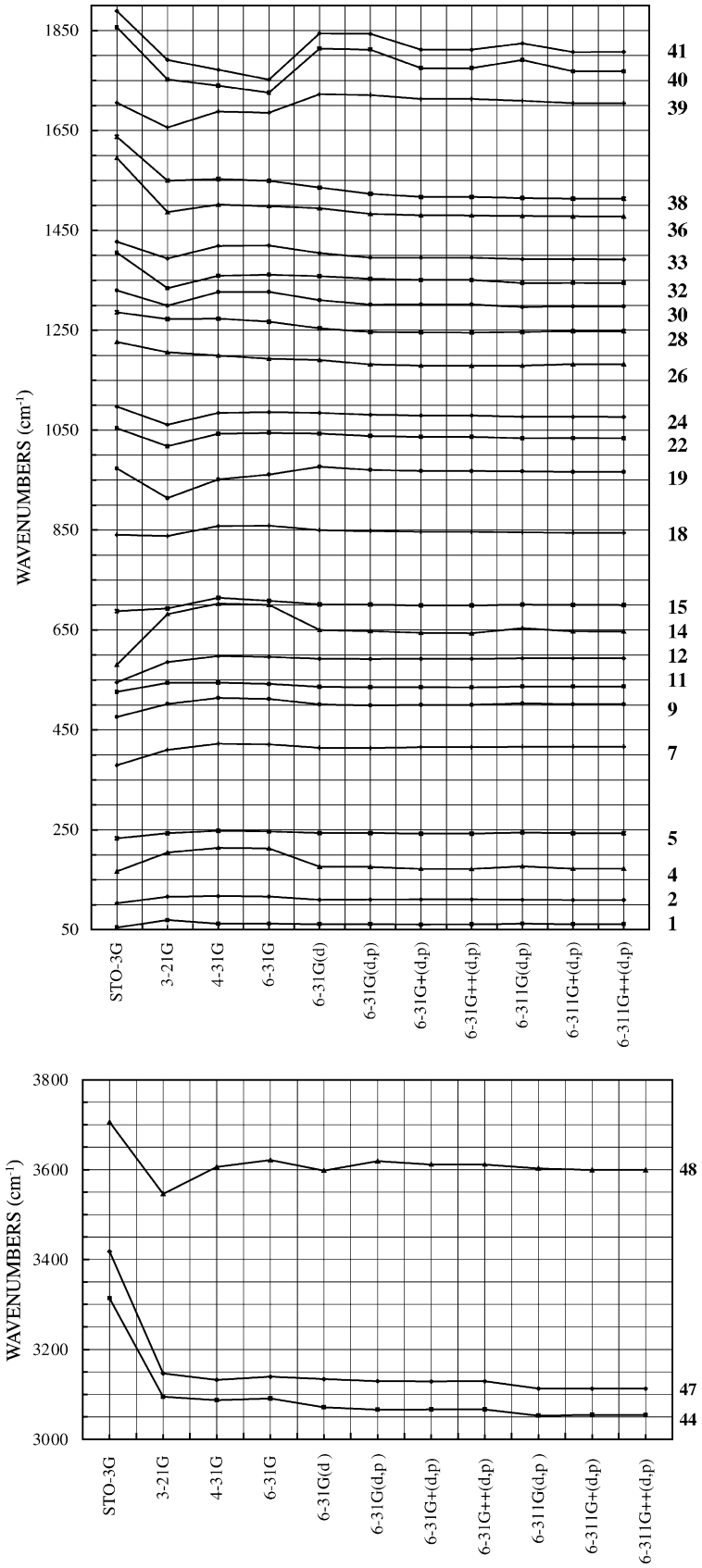


Fig. 8. Basis set effect on some selected fundamental frequencies (vibration modes on the right) in the IR spectrum of bicyclic amidine **1** calculated by B3LYP method.

Table 6
Basis set effect on fundamental frequencies (in $cm^{-1}$) in the IR spectrum of bicyclic amidine **1** calculated by B3LYP method

| Mode | STO-3G | 3-21G | 4-31G | 6-31G | 6-31G(*d*) | 6-31G(*d*, *p*) | 6-31G+(*d*, *p*) | 6-31G++(*d*, *p*) | 6-311G(*d*, *p*) | 6-311G+(*d*, *p*) | 6-311G++(*d*, *p*) |
|---|---|---|---|---|---|---|---|---|---|---|---|
| 1 | 54.2 | 69.5 | 61.7 | 62.0 | 61.0 | 61.1 | 60.4 | 60.6 | 62.0 | 60.9 | 61.1 |
| 2 | 102.8 | 116.1 | 117.3 | 116.3 | 110.0 | 110.3 | 110.5 | 110.4 | 110.0 | 109.6 | 109.7 |
| 3 | 136.2 | 171.6 | 177.1 | 175.6 | 155.6 | 155.8 | 156.5 | 156.4 | 157.2 | 156.7 | 156.7 |
| 4 | 166.5 | 204.6 | 214.0 | 212.8 | 176.0 | 175.7 | 171.9 | 171.6 | 177.1 | 172.2 | 172.1 |
| 5 | 233.1 | 243.1 | 248.0 | 246.5 | 243.6 | 243.3 | 242.6 | 242.5 | 244.6 | 243.0 | 243.0 |
| 6 | 270.4 | 273.4 | 270.7 | 268.8 | 266.1 | 265.2 | 263.2 | 263.3 | 267.0 | 263.9 | 264.0 |
| 7 | 378.9 | 410.0 | 422.4 | 421.0 | 414.0 | 413.8 | 415.5 | 415.4 | 416.3 | 416.5 | 416.5 |
| 8 | 399.1 | 421.0 | 436.2 | 435.7 | 429.0 | 429.0 | 430.2 | 430.1 | 429.5 | 430.0 | 429.9 |
| 9 | 476.0 | 501.8 | 514.2 | 511.9 | 500.8 | 498.9 | 500.3 | 500.2 | 502.9 | 501.2 | 501.2 |
| 10 | 494.7 | 527.4 | 530.3 | 523.4 | 525.9 | 523.8 | 522.8 | 522.2 | 527.7 | 525.1 | 525.0 |
| 11 | 526.2 | 544.0 | 544.6 | 542.0 | 536.3 | 535.5 | 535.3 | 535.3 | 537.0 | 536.8 | 536.8 |
| 12 | 545.1 | 585.7 | 597.8 | 595.9 | 592.1 | 591.9 | 592.2 | 592.1 | 593.4 | 593.5 | 593.4 |
| 13 | 575.2 | 628.5 | 637.9 | 632.1 | 614.1 | 612.8 | 611.2 | 610.8 | 617.5 | 613.9 | 613.7 |
| 14 | 580.5 | 681.9 | 702.6 | 700.2 | 650.0 | 647.6 | 644.1 | 643.5 | 653.9 | 647.4 | 647.1 |
| 15 | 687.8 | 692.9 | 714.4 | 708.6 | 701.4 | 700.9 | 699.3 | 699.2 | 700.9 | 700.1 | 700.0 |
| 16 | 735.6 | 743.1 | 744.0 | 741.1 | 739.6 | 738.9 | 735.6 | 735.7 | 737.4 | 735.5 | 735.5 |
| 17 | 797.8 | 780.4 | 807.7 | 808.5 | 808.2 | 807.2 | 806.8 | 806.7 | 804.6 | 805.0 | 804.9 |
| 18 | 840.2 | 838.0 | 858.2 | 858.8 | 849.8 | 848.0 | 846.8 | 846.8 | 845.3 | 844.6 | 844.6 |
| 19 | 973.2 | 914.1 | 951.6 | 961.1 | 977.0 | 970.6 | 968.6 | 968.2 | 967.6 | 966.5 | 966.2 |
| 20 | 981.8 | 965.0 | 993.8 | 995.4 | 987.9 | 982.3 | 981.8 | 981.3 | 978.8 | 979.0 | 979.0 |
| 21 | 1006.3 | 989.5 | 1017.3 | 1017.4 | 1007.3 | 1000.8 | 998.3 | 998.0 | 997.3 | 996.6 | 996.4 |
| 22 | 1054.0 | 1017.9 | 1042.8 | 1044.4 | 1043.2 | 1038.2 | 1036.7 | 1036.6 | 1034.0 | 1034.1 | 1034.0 |
| 23 | 1063.1 | 1028.5 | 1059.6 | 1060.5 | 1057.3 | 1054.4 | 1053.4 | 1053.3 | 1052.4 | 1052.9 | 1052.8 |
| 24 | 1097.3 | 1061.0 | 1084.7 | 1086.2 | 1084.5 | 1081.0 | 1079.5 | 1079.4 | 1076.8 | 1076.6 | 1076.5 |
| 25 | 1142.6 | 1107.6 | 1133.8 | 1137.9 | 1138.8 | 1136.6 | 1134.3 | 1134.1 | 1126.6 | 1126.7 | 1126.4 |
| 26 | 1226.9 | 1206.1 | 1199.5 | 1192.9 | 1190.7 | 1181.5 | 1179.2 | 1178.8 | 1179.1 | 1181.9 | 1181.8 |
| 27 | 1249.5 | 1219.7 | 1247.4 | 1246.9 | 1231.9 | 1223.4 | 1225.9 | 1225.6 | 1221.7 | 1224.8 | 1224.7 |
| 28 | 1286.1 | 1272.8 | 1273.4 | 1267.4 | 1254.1 | 1246.8 | 1246.0 | 1245.7 | 1246.5 | 1248.5 | 1248.5 |
| 29 | 1310.3 | 1281.2 | 1290.1 | 1286.4 | 1274.3 | 1264.8 | 1263.6 | 1263.8 | 1261.8 | 1263.6 | 1263.7 |
| 30 | 1329.9 | 1299.2 | 1326.6 | 1326.9 | 1310.5 | 1301.4 | 1301.6 | 1301.5 | 1296.6 | 1297.9 | 1297.9 |
| 31 | 1377.1 | 1320.7 | 1344.2 | 1348.1 | 1350.7 | 1344.7 | 1343.3 | 1343.2 | 1335.0 | 1335.3 | 1335.2 |
| 32 | 1405.5 | 1334.1 | 1359.0 | 1361.1 | 1358.6 | 1352.8 | 1350.7 | 1350.7 | 1344.5 | 1344.8 | 1344.6 |
| 33 | 1427.1 | 1393.7 | 1419.0 | 1419.7 | 1404.5 | 1395.3 | 1395.6 | 1395.4 | 1392.3 | 1392.3 | 1392.1 |
| 34 | 1490.0 | 1428.2 | 1450.5 | 1450.8 | 1445.8 | 1440.2 | 1434.0 | 1433.9 | 1430.6 | 1428.0 | 1428.0 |
| 35 | 1540.1 | 1481.0 | 1488.6 | 1484.8 | 1468.5 | 1451.8 | 1443.5 | 1443.2 | 1442.1 | 1440.5 | 1440.4 |
| 36 | 1595.1 | 1486.6 | 1501.6 | 1498.4 | 1494.3 | 1483.1 | 1480.1 | 1480.0 | 1478.8 | 1478.2 | 1478.0 |
| 37 | 1628.2 | 1535.3 | 1538.4 | 1534.4 | 1518.5 | 1504.6 | 1497.7 | 1497.5 | 1496.6 | 1494.7 | 1494.6 |
| 38 | 1637.4 | 1549.7 | 1552.8 | 1549.2 | 1535.6 | 1523.2 | 1516.8 | 1516.8 | 1514.8 | 1513.4 | 1513.3 |
| 39 | 1705.4 | 1655.9 | 1688.3 | 1685.9 | 1722.5 | 1720.9 | 1713.0 | 1713.0 | 1709.6 | 1705.0 | 1704.8 |
| 40 | 1856.7 | 1752.3 | 1739.9 | 1725.9 | 1814.0 | 1812.2 | 1775.0 | 1775.0 | 1791.2 | 1768.6 | 1768.6 |
| 41 | 1889.1 | 1791.2 | 1771.7 | 1752.0 | 1844.5 | 1843.7 | 1812.0 | 1811.8 | 1824.6 | 1807.4 | 1807.6 |
| 42 | 3267.3 | 3013.6 | 3005.9 | 3014.8 | 3006.5 | 3001.5 | 3006.7 | 3006.8 | 2988.0 | 2993.8 | 2993.4 |
| 43 | 3286.5 | 3039.3 | 3040.0 | 3049.0 | 3050.0 | 3045.4 | 3047.3 | 3046.6 | 3029.1 | 3033.3 | 3032.5 |
| 44 | 3314.1 | 3094.6 | 3087.3 | 3091.1 | 3071.7 | 3066.1 | 3066.5 | 3066.6 | 3052.9 | 3054.3 | 3054.1 |
| 45 | 3408.6 | 3136.3 | 3129.2 | 3134.5 | 3107.7 | 3103.4 | 3104.4 | 3104.6 | 3086.3 | 3087.9 | 3087.5 |
| 46 | 3416.6 | 3142.0 | 3129.3 | 3134.8 | 3130.3 | 3125.0 | 3126.7 | 3126.8 | 3111.3 | 3112.2 | 3111.8 |
| 47 | 3418.0 | 3146.4 | 3132.2 | 3139.2 | 3134.0 | 3129.5 | 3128.6 | 3129.1 | 3112.8 | 3112.9 | 3112.9 |
| 48 | 3705.6 | 3546.4 | 3606.2 | 3621.4 | 3598.3 | 3618.9 | 3611.7 | 3611.6 | 3602.6 | 3599.3 | 3599.4 |

*p*). Most of them were split-valence basis sets, where polarization functions (*d* for heavy atoms, *p* for hydrogens) and diffusion functions on both atom types were gradually added. The results are presented in Table 6 and Fig. 8 (for some representative vibration modes). One can see that STO-3G has obvious deficiencies. Compared to the 6-311++G(*d*, *p*) values, some frequencies are strongly overestimated, by 100–200 $cm^{-1}$ (modes 44–48; Fig. 8), whereas others are underestimated (those below 850 $cm^{-1}$). A less irregular behavior can be found for 3-21G, although again, with some rampant over and underestimates through the whole spectral range. The most notable deviations (underestimates) are for the modes involving nitrogen atoms, in particular for modes 48 (NH stretch), 39 (C=N stretch) and 19 (NH deform out-of-plane). The modes with overestimated frequencies are mainly those involving C–H bonds (4, 14, 26–28, 44–47). Further augmenting the basis set to 4-31G and 6-31G increases most frequency values, with an evident exception of C=O stretching modes 40 and 41, exhibiting a low-frequency shift.

The data obtained with 6–31G(*d*) separate the above series of basis sets from larger ones, which show a more uniform behavior. With a few exceptions (for modes 19 and 39–41),

the calculated frequencies tend to decrease with further augmenting the basis set, so that the corresponding scaling factors gradually increase as well. On the other hand, small irregular variations in the calculated wavenumbers persist within the whole basis set range. Thus, we find no convincing arguments to use basis sets larger than 6-31G(*d*) for our purposes.

## Acknowledgements

Financial support from the National Autonomous University of Mexico (grant DGAPA-IN100303) and from the National Council of Science and Technology of Mexico (grant CONACYT-36317-E) is greatly appreciated. F.F.C.-T. would like to thank DGEP UNAM for a fellowship.

## References

[1] V.A. Basiuk, Russ. Chem. Rev. 66 (1997) 187.
[2] D.S. Jones, G.W. Kenner, R.C. Sheppard, Experientia 19 (1963) 126.
[3] D.S. Jones, G.W. Kenner, J. Preston, R.C. Sheppard, Tetrahedron 21 (1965) 3209.
[4] K. Titlestad, Chemistry and Biology of Peptides, in: The 3rd American Peptide Symposium, Ann Arbor Science, Michigan, 1972, p. 59.
[5] M.Y. Ali, J. Dale, K. Titlestad, Acta Chem. Scand. 27 (1973) 1509.
[6] M. Rothe, M. Fahnle, R. Pudill, W. Schindler, in: E. Gross, J. Meienhofer (Eds.), Peptides: Structure and Biological Function, Pierce Chemical Co., Rochford, 1979, p. 285.
[7] M.Y. Ali, A. Khatun, Tetrahedron 41 (1985) 451.
[8] M.Y. Ali, Protein Structure–Function, in: Proceedings of the International Symposium, TWEL Publishers, Karachi, 1990, p. 209.
[9] T. Yamada, A. Iwamoto, T. Yanagi, T. Miyazawa, S. Kuwata, M. Saviano, V. Pavone, in: Y. Okada (Ed.), Peptide Chemistry 1993, Protein Research Foundation, Osaka, 1993, p. 65.
[10] M. Saviano, A. Lombardi, V. Pavone, T. Yamada, T. Yanagi, A. Iwamoto, S. Kuwata, Acta Cryst. C 52 (1996) 1705.
[11] V.A. Basiuk, J. Anal. Appl. Pyrol. 47 (1998) 127.
[12] V.A. Basiuk, R. Navarro-González, Icarus 134 (1998) 269.
[13] V.A. Basiuk, R. Navarro-González, E.V. Basiuk, J. Anal. Appl. Pyrol. 45 (1998) 89.
[14] V.A. Basiuk, R. Navarro-González, J. Chromatogr. A 776 (1997) 255.
[15] V.A. Basiuk, R. Navarro-González, E.V. Basiuk, Russ. J. Bioorg. Chem. 24 (1998) 747.
[16] V.A. Basiuk, L. Van Meervelt, V.A. Soloshonok, E.V. Basiuk, Acta Cryst. C 56 (2000) 598.
[17] H. Strasdeit, I. Busching, S. Behrends, W. Saak, W. Barklage, Chem. Eur. J. 7 (2001) 1133.
[18] V.A. Basiuk, Spectrochim. Acta A 55 (1999) 289.
[19] V.A. Basiuk, Spectrochim. Acta A 57 (2001) 1271.
[20] V.A. Basiuk, Spectrochim. Acta A 59 (2003) 1867.
[21] M.W. Wong, Chem. Phys. Lett. 256 (1996) 391.
[22] A.P. Scott, L. Radom, J. Phys. Chem. 100 (1996) 16502.
[23] M.D. Halls, H.B. Schlegel, J. Chem. Phys. 109 (1998) 10587.
[24] V.A. Basiuk, T. Yu Gromovoy, A.A. Chuiko, V.A. Soloshonok, V.P. Kukhar, Synthesis (5) (1992) 449.
[25] V.A. Basiuk, J. Douda, Planet. Space Sci. 47 (1999) 577.
[26] J. Douda, V.A. Basiuk, J. Anal. Appl. Pyrol. 56 (2000) 113.
[27] M.J. Frisch, G.W. Trucks, H.B. Schlegel, G.E. Scuseria, M.A. Robb, J.R. Cheeseman, V.G. Zakrzewski, J.A. Montgomery Jr., R.E. Stratmann, J.C. Burant, S. Dapprich, J.M. Millam, A.D. Daniels, K.N. Kudin, M.C. Strain, O. Farkas, J. Tomasi, V. Barone, M. Cossi, R. Cammi, B. Mennucci, C. Pomelli, C. Adamo, S. Clifford, J. Ochterski, G.A. Petersson, P.Y. Ayala, Q. Cui, K. Morokuma, D.K. Malick, A.D. Rabuck, K. Raghavachari, J.B. Foresman, J. Cioslowski, J.V. Ortiz, A.G. Baboul, B.B. Stefanov, G. Liu, A. Liashenko, P. Piskorz, I. Komaromi, R. Gomperts, R.L. Martin, D.J. Fox, T. Keith, M.A. Al-Laham, C.Y. Peng, A. Nanayakkara, C. Gonzalez, M. Challacombe, P.M.W. Gill, B. Johnson, W. Chen, M.W. Wong, J.L. Andres, C. Gonzalez, M. Head-Gordon, E.S. Replogle, J.A. Pople, Gaussian 98W, Revision A. 7, Gaussian, Inc., Pittsburgh, PA, 1998.
[28] E.V. Basiuk, V.A. Basiuk, J.-G. Bañuelos, J.-M. Saniger-Blesa, V.A. Pokrovskiy, T.Yu. Gromovoy, A.V. Mischanchuk, B.G. Mischanchuk, J. Phys. Chem. B 106 (2002) 1588.
[29] V.A. Basiuk, E.V. Basiuk, J.-M. Saniger-Blesa, Nano Lett. 1 (2001) 657.
[30] V.A. Basiuk, J. Phys. Chem. B 107 (2003) 8890.